AD-A037 193 WESTINGHOUSE DEFENSE AND ELECTRONIC SYSTEMS CENTER B--ETC F/G 20/5
CAVITY DUMP-PTM ND:LASER.(U)
JAN 77 J L WENTZ, G D BALDWIN F33615-74-C-1011

UNCLASSIFIED AFAL-TR-75-214 NL

1 OF 1
ADA037193

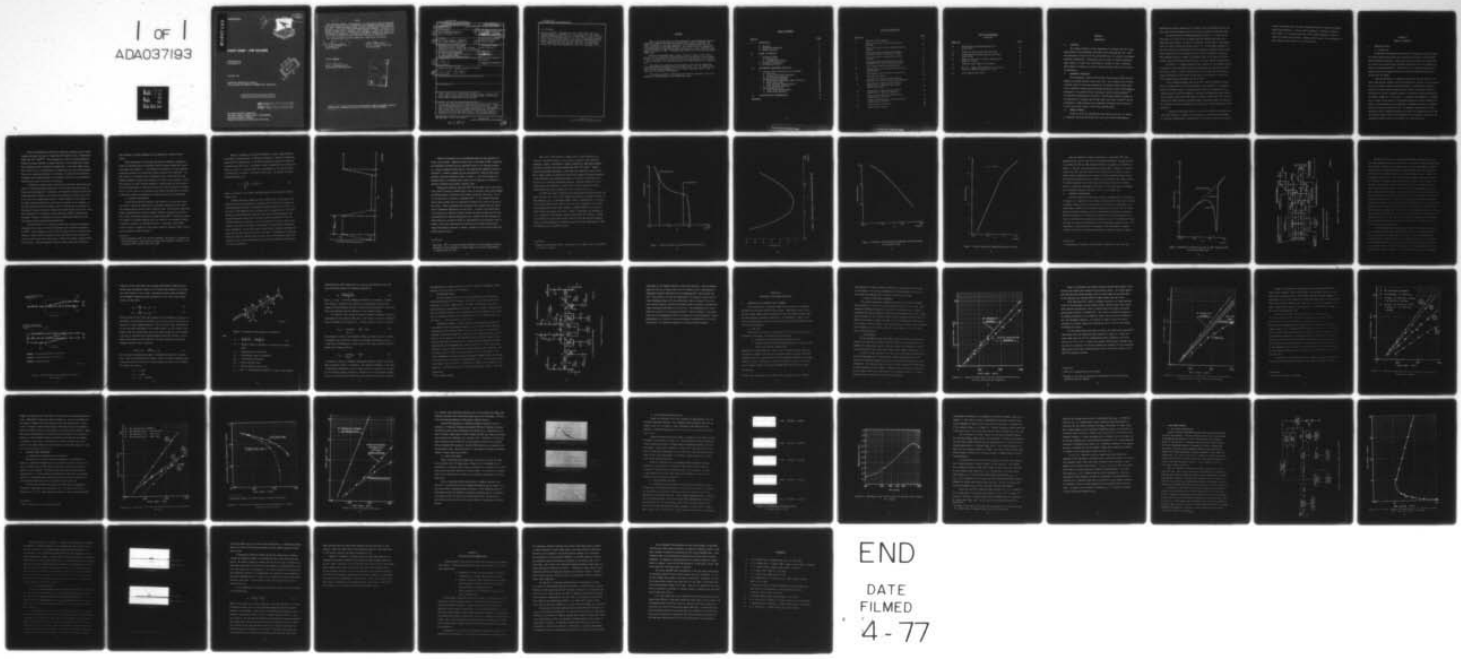

END

DATE
FILMED
4-77

AFAL-TR-75-214

12

CAVITY DUMP - PTM Nd:LASER

WESTINGHOUSE
BALTIMORE, MD

JANUARY 1977

TECHNICAL REPORT AFAL-TR-75-214
FINAL REPORT FOR PERIOD: NOVEMBER 1973 - MARCH 1975

AIR FORCE AVIONICS LABORATORY
AIR FORCE WRIGHT AERONAUTICAL LABORATORIES
AIR FORCE SYSTEMS COMMAND
WRIGHT-PATTERSON AIR FORCE BASE, OHIO 45433

NOTICE

When Government drawings, specifications, or other data are used for any purpose other than in connection with a definitely related Government procurement operation, the United States Government thereby incurs no responsibility nor any obligation whatsoever; and the fact that the government may have formulated, furnished, or in any way supplied the said drawings, specifications, or other data, is not to be regarded by implication or otherwise as in any manner licensing the holder or any other person or corporation, or conveying any rights or permission to manufacture, use, or sell any patented invention that may in any way be related thereto.

This technical report has been reviewed and is approved for publication.

Mr. Michael M. Hell
Project Engineer

Dr. R. F. Paulson, Acting Chief
E-O Sources Group

FOR THE COMMANDER

W. C. Schoonover
Mr. W. C. Schoonover, Chief
Electro-Optics Technology Branch

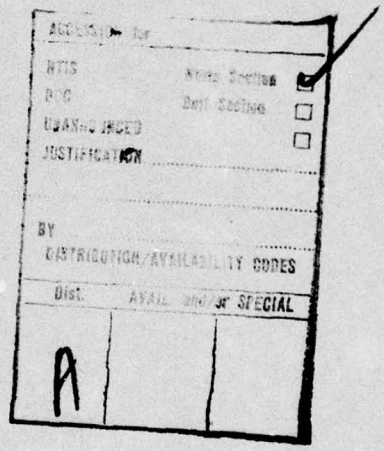

Copies of this report should not be returned unless return is required by security considerations, contractual obligations, or notice on a specific document.

AIR FORCE - 7 MARCH 77 - 100

Unclassified

SECURITY CLASSIFICATION OF THIS PAGE (When Data Entered)

REPORT DOCUMENTATION PAGE	READ INSTRUCTIONS BEFORE COMPLETING FORM
1. REPORT NUMBER: AFAL-TR-75-214	2. GOVT ACCESSION NO. / 3. RECIPIENT'S CATALOG NUMBER
4. TITLE (and Subtitle): CAVITY DUMP-PTM Nd:LASER	5. TYPE OF REPORT & PERIOD COVERED: Final Report for Period: Nov 73 — Mar 75
	6. PERFORMING ORG. REPORT NUMBER
7. AUTHOR(s): John L. Wentz and Gary D. Baldwin	8. CONTRACT OR GRANT NUMBER(s): F33615-74-C-1011
9. PERFORMING ORGANIZATION NAME AND ADDRESS: Westinghouse Electric Corporation, Defense & Electronic Systems Center, Systems Development Division, P.O.Box 746, Balt.,Md.21203	10. PROGRAM ELEMENT, PROJECT, TASK AREA & WORK UNIT NUMBERS: Project 2001/Task 01
11. CONTROLLING OFFICE NAME AND ADDRESS: Air Force Avionics Laboratory, Air Force Wright Aeronautical Laboratories, Air Force Systems Command, Wright-Patterson Air Force Base, Ohio	12. REPORT DATE: Jan 1977
	13. NUMBER OF PAGES: 54
14. MONITORING AGENCY NAME & ADDRESS (if different from Controlling Office): 61 p.	15. SECURITY CLASS. (of this report): Unclassified
	15a. DECLASSIFICATION/DOWNGRADING SCHEDULE

16. DISTRIBUTION STATEMENT (of this Report)

Approved for Public Release; Distribution Unlimited.

16: 2001 17: 01

17. DISTRIBUTION STATEMENT (of the abstract entered in Block 20, if different from Report)

18. SUPPLEMENTARY NOTES

19. KEY WORDS (Continue on reverse side if necessary and identify by block number)

lasers, crystal lasers, birefringence, Nd:doped crystals, Q-switched laser, optical pumping, cavity dumping, pulse transmission mode, high PRF, high average power, extended pulse transmission mode

20. ABSTRACT (Continue on reverse side if necessary and identify by block number)

Three major areas have been investigated with regard to obtaining high PRF/high average power operation from a solid state YAG:Nd laser: 1) application of high speed electro-optic modulation techniques to a high average power low gain laser device; 2) temporal modulation format required to obtain stable and efficient pulsed operation at PRF's between the classically accepted PTM and Cavity Dump (CD) frequency limits; 3) pulsed operation of DC Krypton arc lamp at 10 Hz (25% duty cycle) and subsequent pulse burst

DD FORM 1 JAN 73 1473 EDITION OF 1 NOV 65 IS OBSOLETE

Unclassified

SECURITY CLASSIFICATION OF THIS PAGE (When Data Entered)

CONTINUED

405897

Y/B

20. (continued)

lasing at high PRF's. Employment of a dual crystal Pockels cell, fast switching modulator electronics with a variable duty cycle, and a hybrid resonator configuration has resulted in the attainment of stable Q-switched pulse trains over the PRF range of 0.1 to 1 MHz. During pulsed operation, overall efficiency was 85% of the CW maximum value, pulsewidth was 40 nanoseconds, pulse amplitude stability better than ± 10%, and average power levels exceeding 10 watts were obtained. Over the 0.1 to 1 MHz range, average output power and pulsewidth were found to be independent of PRF.

FOREWARD

This is the final report on work performed at the Westinghouse Electric Corporation, Defense and Electronics System Center (DESC), Baltimore, Md. 21203, to develop a very high repetition rate neodymium doped solid state laser operating with coupling modulation. The objective of this program was to obtain narrow width Q-Switched pulse emission over a pulse repetition rate range of 100 KHZ to 1 MHZ. An average power output of 25 watts was the system design goal.

Work was accomplished under Contract F33615-74-C-1011, Project 2001/ Task 01, for the Electronic Technology Division, Electro-Optics Device Branch, of the Air Force Avionics Laboratory (AFSC) under the guidance of Mr. Michael M. Heil, AFAL/DHO-1, the contracting officer's designated technical representative.

This report was submitted by the authors in June 1975 and summarizes work done between 15 November 1973 and 15 March 1975. Mr. C.R. Kline, Manager, Electro-Optics System Department was the Project Supervisor and Mr. John L. Wentz was the Principal Investigator.

The authors gratefully acknowledge the technical assistance of Dr. R.W. Rampolla in various phases of the experimental work.

TABLE OF CONTENTS

LIST OF ILLUSTRATIONS

LIST OF ILLUSTRATIONS

(continued)

SECTION I

INTRODUCTION

1. OBJECTIVE

The primary objective of this program was to construct and test a very high repetition rate Q-Switched Solid State Laser employing YAG: Nd. Laser pump excitation in both the DC and pulsed modes was to be studied to determine parametric dependencies. Design goals were to obtain an average Q-Switched power output of 25 watts over a PRF range of 100 KHZ to 1 MHZ. Individual pulse widths, as measured at the half intensity points, were to be less than 50 nanoseconds.

2. BACKGROUND INFORMATION

The Westinghouse Defense and Electronic Systems Center (DESC) has been engaged in building military lasers since 1965. This experience has provided a valuable basis for the work performed on the present contract which represents a wedding of several laser techniques previously studied at Westinghouse. Development of an airborn CW laser employing a spherical pump geometry,[1,2] acoustic-optic Q-Switching of CW lasers,[3] electro-optic modulator design and its application to low gain high average power solid state lasers,[4,5] and investigations of high frequency laser modulation techniques have directly influenced the overall design of the Cavity Dump-PTM laser.

3. GENERAL APPROACH

Design of the Cavity Dump-PTM laser was based on the use of a number of components which had previously been built and tested by Westinghouse.

Combining these basic elements into a workable high PRF Q-Switched laser, however, had not been attempted prior to the start of contract F33615-74-C-1011.

The basic CW laser configuration, which includes a 5 x 50 mm YAG: Nd laser rod, a 5 mm bore 50 mm arc length 3000 Torr Krypton pump lamp, and a spherical pump enclosure is capable of producing CW power outputs exceeding 70 watts at overall efficiencies greater than 2.5%. Electro-Optic modulation of the laser emission is accomplished via a Westinghouse transverse field polarization modulator used in conjunction with a calcite polarization separator. This modulator design is capable of switching times on the order of 10 nanoseconds, with the limiting factor being the electronic driver switching speed.

By virtue of a charge/discharge design concept, the E/O modulator driver is capable of rapid switching between the high-to-low and low-to-high Q resonant cavity states. Control capability has been designed into the driver to permit flexibility in the choice of PRF, high Q time period at a given PRF, and resonator output coupling in the low Q state.

Laser resonator geometry employs two flat totally reflecting mirrors. With no voltage applied to the E/O modulator, laser radiation is constrained within the resonant cavity. Resonator output coupling is dependent on the voltage applied to the E/O modulator. Using this configuration, laser modulation essentially follows the PTM format as defined by Vuylsteke[11] with the exception that photon density, during the high Q laser pulse build up period, is not permitted to reach its natural peak value prior to being coupled out of the resonator.

A single arc lamp power supply is used for CW and 10 Hz/25 percent duty cycle pump operation. Included in this supply is a starting circuit capable of imposing a high-voltage of approximately 25 kilovolts across the arc lamp to

initiate ionization and a low power sustaining circuit to maintain ionization during lamp operation. A series current regulator is employed to regulate lamp current. In the pulsed mode, the series current regulator is gated to obtain the desired pulse current. Between current pulses, the sustaining circuit maintains lamp ignition at a low power level.

SECTION II

THEORY OF OPERATION

1. MODULATION THEORY

a. Introduction

Considerable experimental and theoretical investigation has been directed toward obtaining sequential pulse operation from lasers utilizing intracavity modulation techniques. Early work involved internal loss modulation[6], but it was soon recognized that bandwidth limitations made this technique inferior to coupling modulation[7]. Through the use of coupling modulation, sequential pulses from low-gain He-Ne lasers have been generated over an extremely wide PRF range[8].

Coupling modulation, as originally proposed by Gurs and Muller[7], requires that coherent energy in the laser resonator be coupled out of the cavity via a time variable output coupling reflectance. Implementation generally utilizes a resonant cavity formed by two 100 percent reflecting mirrors between which is placed a modulator capable of directing a predetermined amount of coherent energy out of the cavity. In general, the modulator is initially set to couple out the amount of circulating energy which yields maximum efficiency. Pulsed operation is accomplished by swinging the degree of coupling above and below this quiescent level. An important characteristic of this particular form of coupling modulation, as applied to low-gain lasers, is that the coherent photon density in the resonator is not allowed to decay into the spontaneous emission noise level between each successive pulse.

Chesler and Maydan have described a modulation technique called "Cavity Dumping" which has been used to obtain high PRF operation from a continuously pumped YAG: Nd^{+3} laser[9,10]. This technique is a form of coupling modulation wherein the output coupling is varied from zero to some minimum value rather than modulating around a quiescent coupling level. For cavity dumped (hereafter referred to as CD) modulation, no energy exits the cavity except during the time the coupling reflectance is a minimum. As with the Gurs and Muller technique, cavity photon density is not allowed to decay into the spontaneous emission noise level at the end of each pulse.

To maintain a constant power efficiency, CD operation requires that the amount of circulating energy coupled out of the cavity during each pulse increase with decreasing PRF. Eventually a limiting PRF is reached at which the circulating photon density is just above the spontaneous emission noise level at the end of the coupling time period. Further reduction in PRF results in the photon density decaying into noise and the cessation of CD operation. It has been postulated that CD operation below the limiting PRF is possible by adjusting the output coupling to maintain the photon density above noise. Computer simulation of CD operation by the authors has further confirmed this postulate. However, CD modulation below the limiting PRF produces an efficiency which rapidly drops with decreasing PRF.

As early as 1961, A. A. Vuylsteke pointed out a method of operating a Q-Switched laser known as the Pulse Transmission Mode (hereafter referred to as PTM)[11]. This technique also falls into the generic class of coupling modulation, it differs from CD operation in that the coherent photon density decays into noise at the end of each pulse. However, the output coupling follows the CD format. Although originally directed toward single pulse operation,

this technique is readily adaptable to the generation of high PRF pulse trains.

Under conditions of CW pumping, PTM operation exhibits a gradual decrease in efficiency when the interpulse period increases beyond the fluorescent decay time constant τ. This behavior is governed by the same physical constraints observed in conventional pulsed reflection mode operation[3]. For PRF's below $1/\tau$, efficiency can be maintained only if short duration pulse pumping techniques, using a pulse duration less than τ, are employed. As the PRF increases, an upper limiting frequency is reached when the time required for the photon density to build up from the noise level and attain its maximum value is on the order of an interpulse time period; PTM operation, as defined by Vuylsteke, cannot be maintained at frequencies above this limiting PRF.

b. Extended PTM Operation

CD and PTM modulation techniques, when applied to a particular laser, each cover a limited PRF range which is dependent principally on the active laser medium employed and the pump excitation level. PTM operation efficiently produces sequential pulses from a minimum frequency, determined by τ and the type of pump excitation employed, to an upper limit ν_1/PTM. Efficient CD operation begins at a minimum frequency ν_1/CD and extends to some maximum PRF which is normally limited by the modulation device. In general, $\nu_1/\text{CD} > \nu_1/\text{PTM}$, so that a range of frequencies exists where efficient operation cannot be provided by either the PTM or CD mode.*

---

* Pulsed reflection mode[11] has an upper frequency limit which is somewhat less than the PTM limit. Thus, pulsed reflection mode modulation cannot be used to generate PRF's between ν_1/CD and ν_1/PTM.

Figure 1 illustrates the temporal variation in output coupling reflectance which is characteristic of PTM and CD operation. Effective reflectivity varies from its maximum value of 100 percent during the high Q time period to a minimum low Q value of R_o. We assume a fixed Q transition time for the modulator, t_1, and $(t_3 - t_2)$, but allow the low Q period $(t_4 - t_3)$ and the depth of modulation R_o to vary as a function of PRF $(1/t_4)$. We proceed to define a coupling function f_c as

$$f_c = \int_{t_2}^{t_5} \left[1 - R_o(t)\right] dt \qquad (1)$$

which is a measure of the output coupling capacity of the modulator during a single cycle.

Constant amplitude sequential pulse operation (at a fixed pump level) requires that the time variation of inversion in the active laser medium and circulating photon density be identically reproduced from pulse to pulse. In the case of PTM operation, this is rather easy to accomplish since the photon density is in the spontaneous emission noise level at the beginning of the pulse build-up time (end of the low Q time period) and this noise level is a direct function of inversion. It is thus possible to select a value of inversion at the start of the pulse train which will produce amplitude equilibrium immediately. On the other hand, steady state CD operation maintains the photon density above the noise level at all times. Consequently, CD amplitude stability cannot be obtained with the first pulse of the sequence (which must obviously build from the spontaneous noise level) but requires multiple pulses to achieve equilibrium.

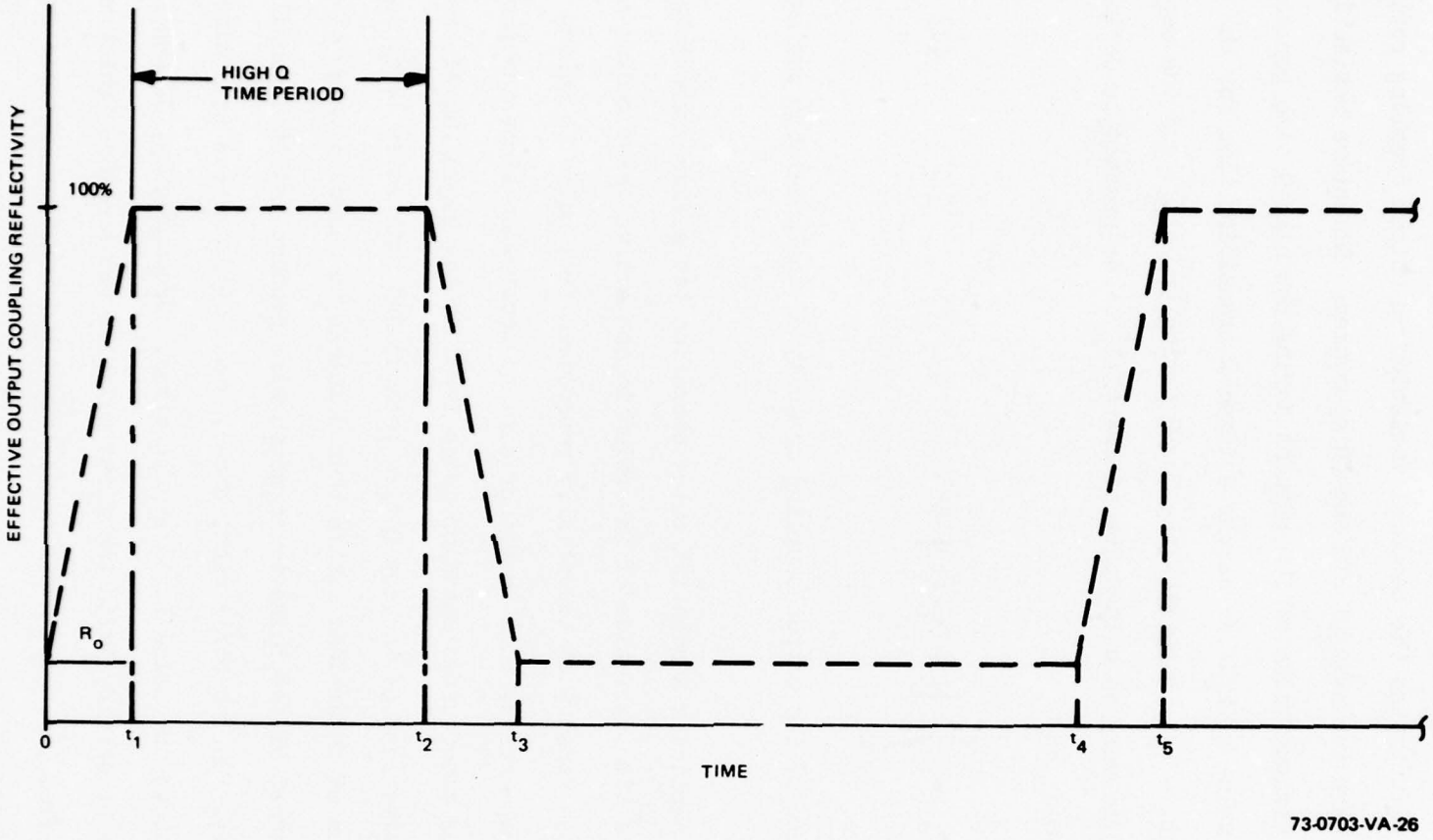

Figure 1 Modulator Timing Sequence

PTM and CD operation can be accomplished using the same physical resonant cavity design. Operation differs only in the range of PRF's covered by each modulation technique and the applicable value of the coupling function f_c. Using a slightly modified form of the computational approach outlined in reference[3], a computer program has been implemented to study multiple pulse operation using the modulation format in figure 1. With this program, the characteristics of sequential pulse trains can be obtained as a function of resonator parameters and initial inversion level.

Computations obtained using YAG: Nd^{+3} and CaLa SOAP: Nd^{+3} as the active laser medium* initially confirmed that a mode of operation exists which bridges the PRF gap between ν_1/PTM and ν_1/CD without sacrificing efficiency. We refer to this mode of operation as "Extended PTM." In the Extended PTM mode, photon density decays into the spontaneous emission noise level at the end of each pulse. Stable sequential pulse operation thus requires that the inversion be reproduced identically for each cycle. In order to accomplish this, it is necessary to maintain a balance between the peak inversion and the peak circulating photon density during each cycle. Whereas for PTM operation the photon density is allowed to build up, unrestricted by the modulator, until it reaches a peak value consistent with cavity losses and peak inversion, Extended PTM operation switches or "dumps", energy out of the cavity before this natural peak can occur.

---

* CaLa SOAP: Nd^{+3} is a laser material developed at the Westinghouse Research Laboratories which exhibits an energy storage per unit gain approximately 5 x greater than YAG: Nd^{+3}.

Each value of PRF requires a unique value of peak inversion at t_4 (Figure 1) and photon density at t_2 in order to maintain pulse amplitude stability. Figure 2 illustrates a typical variation in peak photon density with PRF as obtained for a pulse pumped CaLa SOAP: Nd^{+3} laser.* Figure 3 shows the associated dependence of peak inversion during each cycle on PRF while figure 4 gives the difference between the maximum and minimum inversion. As PRF increases, the percentage variation in inversion is drastically reduced due to a decreased peak photon density. Inversion remains at a reasonably high level, however, to ensure that the photon density can build sufficiently from noise to achieve the required peak value at t_2.

At PRF's just above ν_1/PTM, the time during which the photon density remains in noise, $(t_4 - t_3)$ is just slightly less than the interpulse period. As PRF increases, $(t_4 - t_3)$ decreases until a point is reached where f_c is sufficiently small that the time spent in the noise level approaches zero. Efficient operation above this point requires a further reduction in f_c and the photon level never decays into noise. Figure 5 illustrates the variation in f_c as a function of PRF obtained using the CaLa SOAP: Nd^{+3} example. Referring to figure 2, we find that for PRF's below 300 KHZ Extended PTM operation blends into PTM operations as defined by Vuylsteke; above approximately 5 MHz, the transition to CD operation occurs.

---

* Pumping is accomplished using a square pump pulse 100μsec long and containing 7.3 joules of energy.

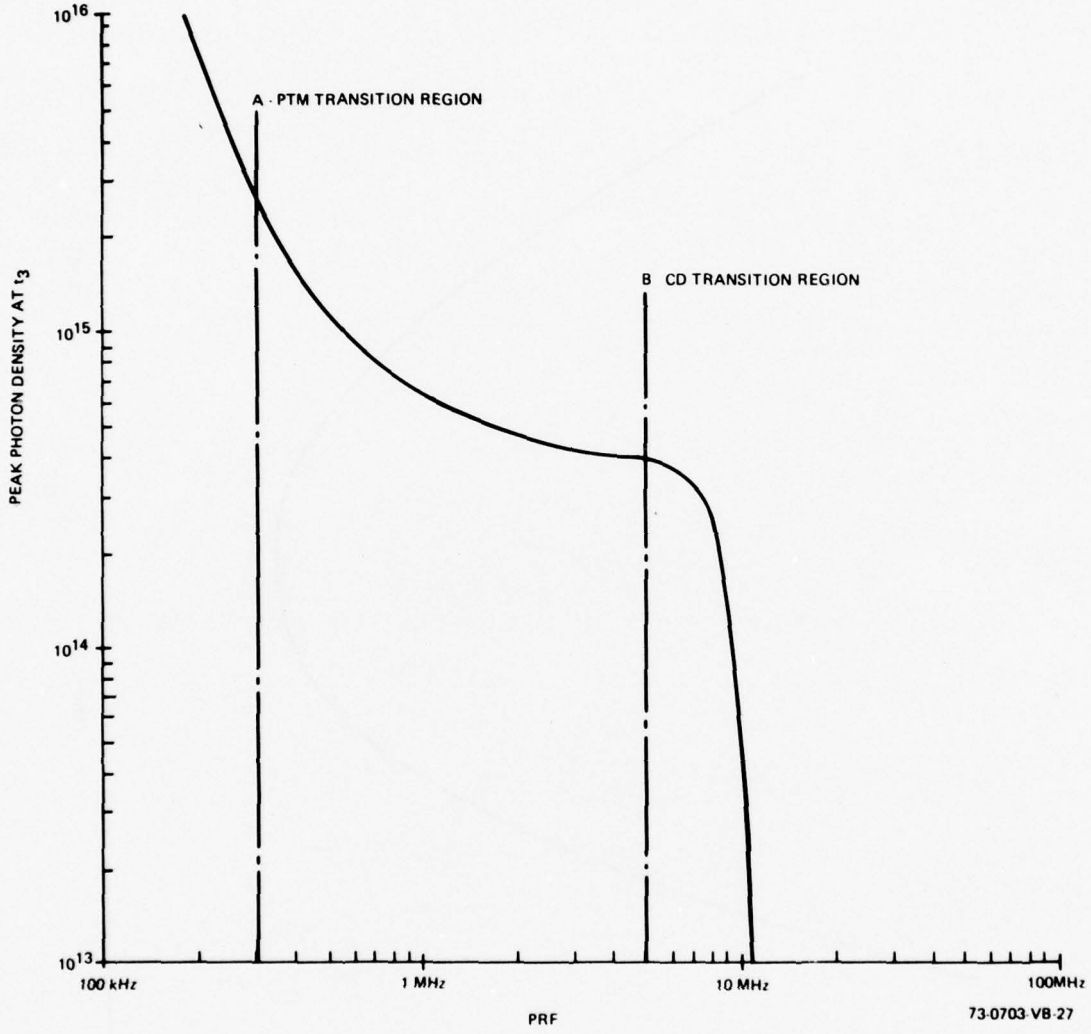

Figure 2 Typical Variation in Peak Photon Density with PRF

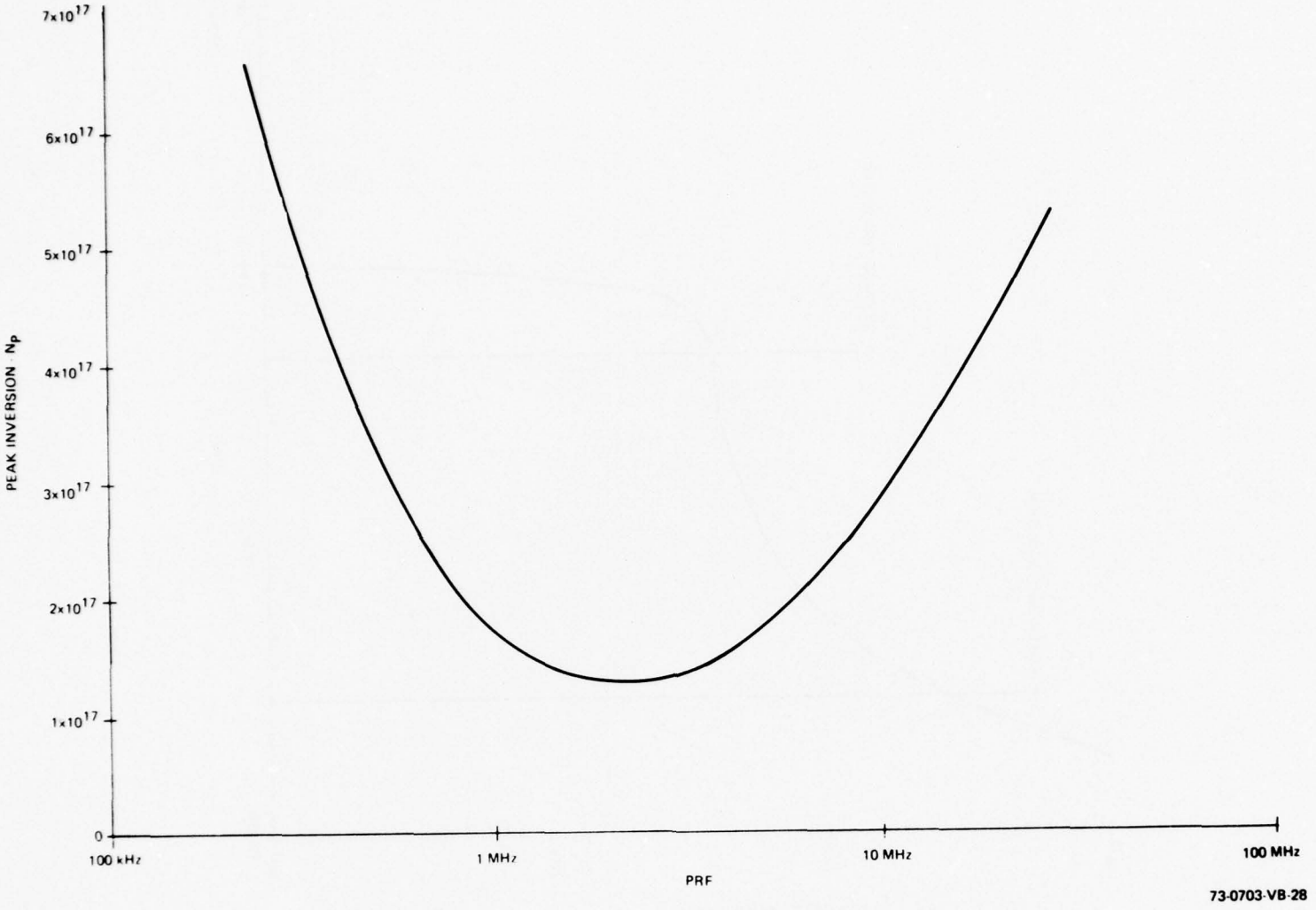

Figure 3 Typical Variation in Peak Inversion Density with PRF

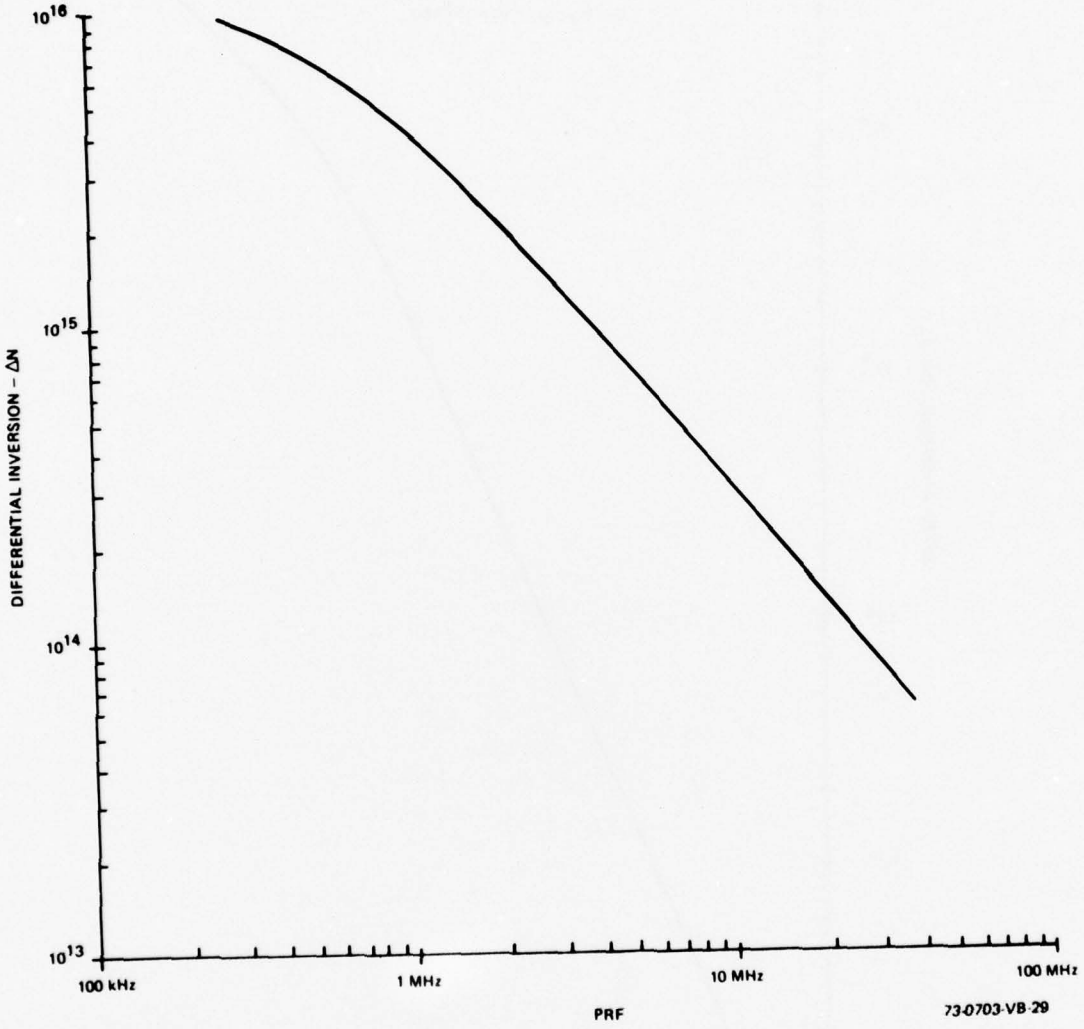

Figure 4 Difference Between Maximum and Minimum Inversion Density as a Function of PRF

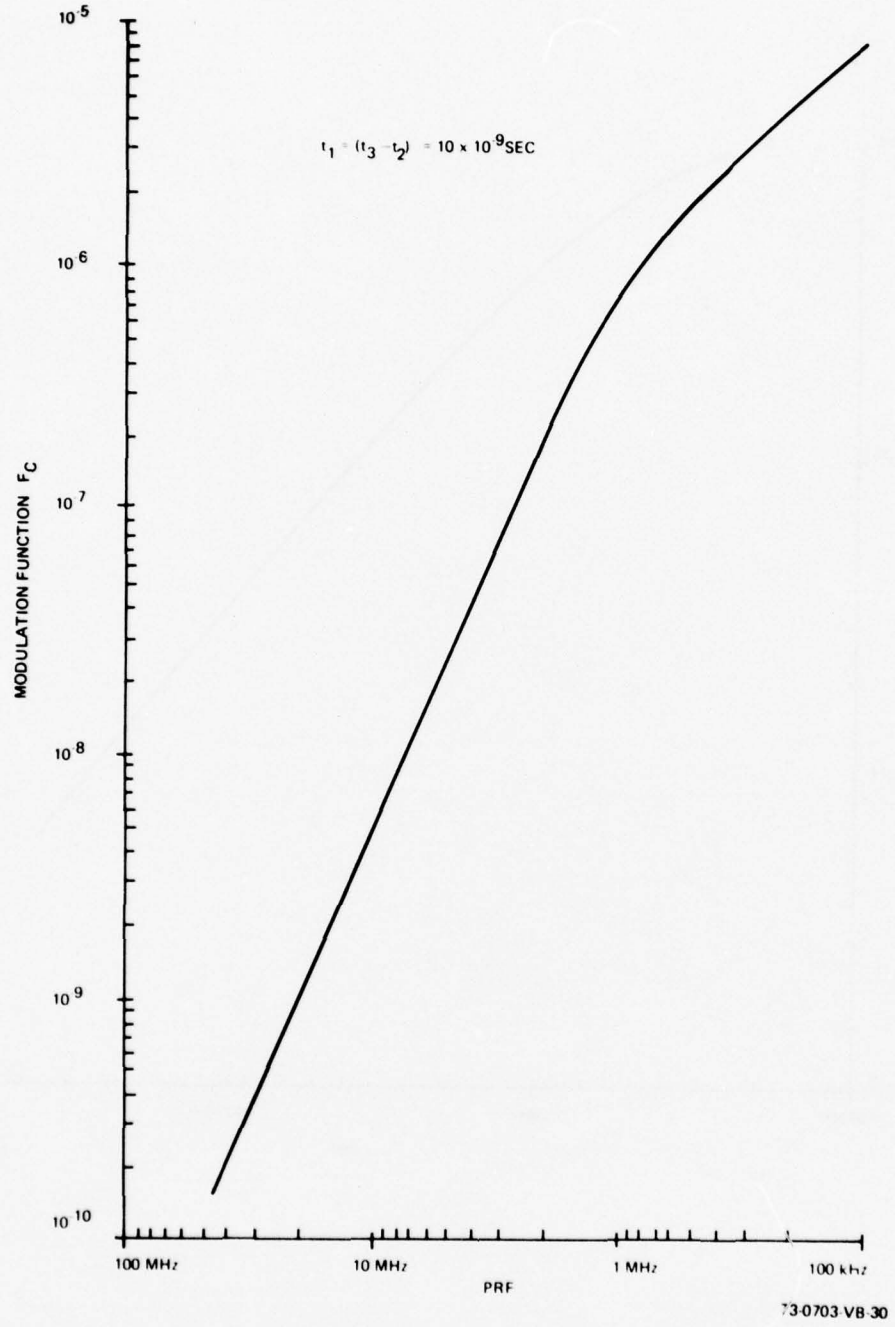

Figure 5 Typical Variation in Modulation Function with PRF

Data was obtained to compare efficiency of a CaLa SOAP: Nd^{+3} laser operating below ν_1/CD in both the CD and Extended PTM modes. Energy per pulse as a function of PRF for PTM, Extended PTM and CD operation is illustrated in figure 6. From the preceding discussion and the data in figure 6, it becomes obvious that PTM, "Extended" PTM, and CD modulation can be employed using a common cavity configuration (See Section II.2) and modulation format to provide efficient sequential pulse emission over an extremely wide range of PRF's. Of further importance is the fact that the temporal width of each emitted pulse is essentially independent of PRF and is of the same order of magnitude as the coupling transition time [t_1 or $(t_3 - t_2)$ in figure 1].

2. RESONATOR CONFIGURATION

The basic Cavity Dump-PTM laser resonator configuration, as illustrated in figure 7, is comprised of two totally reflecting mirrors which form the high Q resonant cavity, an active laser medium in the form of a cylindrical rod, a polarization separator for resolving an unpolarized laser beam into two orthogonally polarized components, and an electro-optical polarization modulator. Efficient operation of a laser, in the presence of strong depolarization effects in the active laser medium*, necessitates the use of a modulation technique which can operate simultaneously on two orthogonally polarized beams. This requirement is satisfied by the combination of the polarization separator (element B) and the E/O polarization modulator (element QS) shown in figure 7.

---

* Depolarization is produced by thermo-optic distortion in the laser rod.

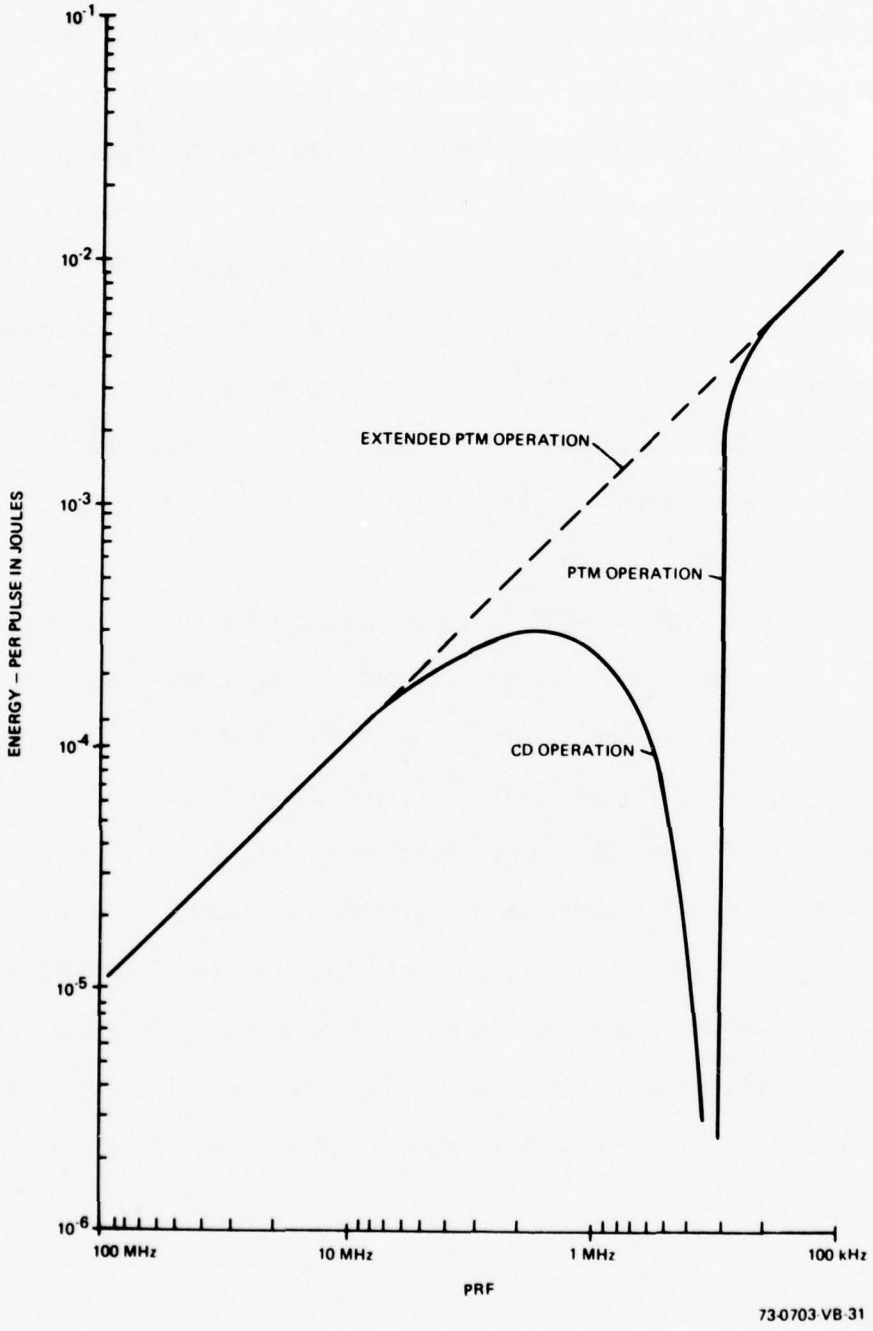

Figure 6 Energy/Pulse Variation with PRF for PTM, "Extended" PTM and CD Operational Modes

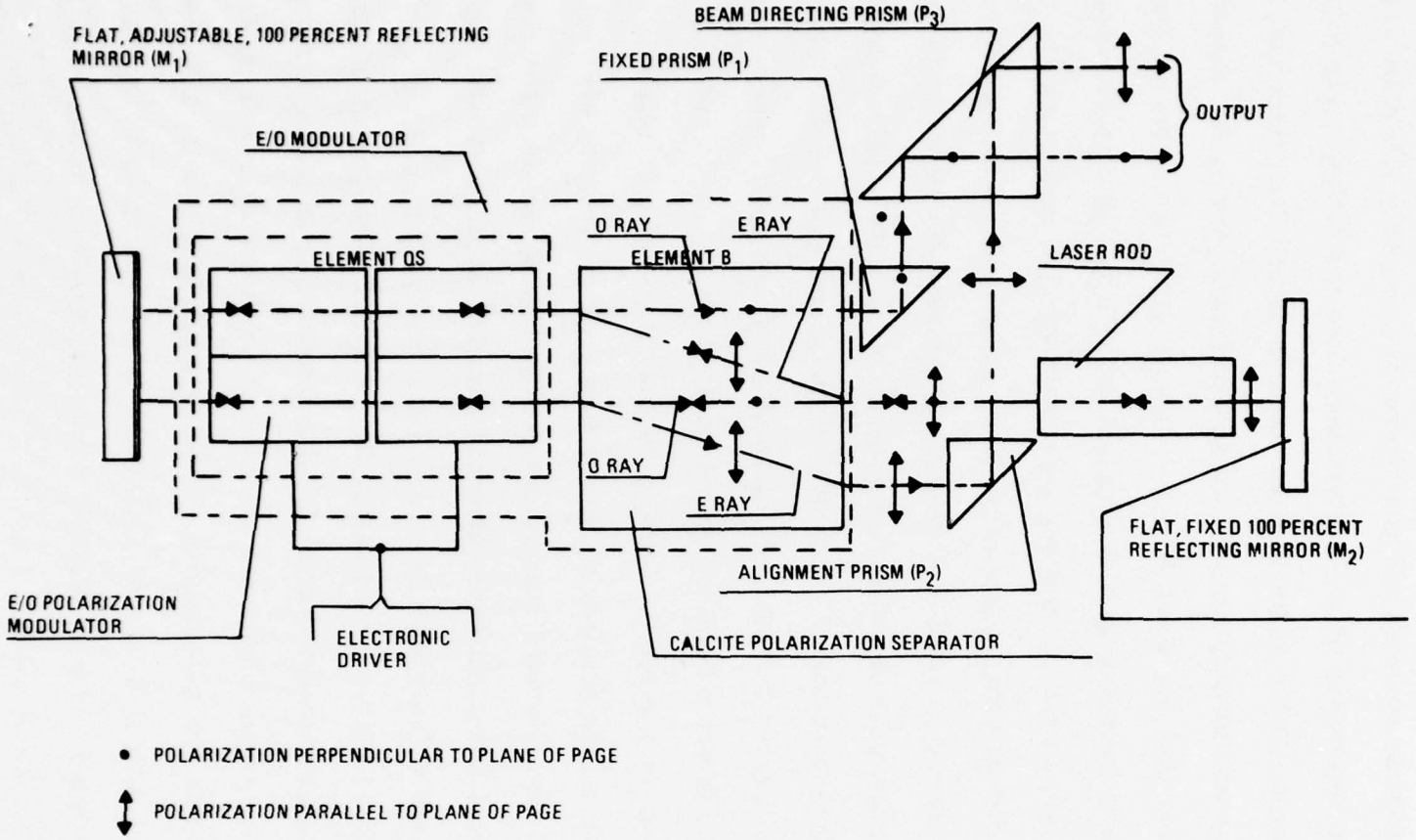

Figure 7 Cavity Dumped Resonator Configuration

Element B consists of an optically birefringent material such as calcite; when properly oriented and positioned in a randomly polarized light beam, it will cause separation of an incident beam into two orthogonally polarized components due to double refraction as shown in figure 8A. These components are denoted as an ordinary ray, O, and an extraordinary ray, E. Element B is configured such that the O and E rays emerge as parallel components separated by a distance D dependent upon the optical path length of this element. If no change occurs in the O and E ray polarization, upon reflecting the beams back through the element, they will retrace their original paths and recombine as they emerge to produce a randomly polarized beam as shown in figure 8A. Laser oscillation will occur for this state since optical feedback is allowed along the laser rod axis. If each of the orthogonal polarization components is rotated 90 degrees by the E/O polarization modulator, QS, prior to reentering element B, the two rays will not retrace their original paths and will follow the paths shown in figure 8B. This is because the 90-degree rotation of polarization results in the original O ray becoming an E ray and the original E ray becoming an O ray. In this state, laser energy is coupled from the resonator via two parallel beams which are directed parallel to the resonator axis by prism P_1,P_2, and P_3 of figure 7.

The E/O polarization modulator, QS, consists of two potassium dideuterium phosphate electro-optic crystals with orientation as shown in figure 9. The axes shown in this figure are the axes of the index ellipsoid when an electric field is applied along the Z (or crystal optic) axes. The crystals are orientated with their Z axes transverse to the optical path and perpendicular to each other. For an incident light beam linearly polarized at 45 degrees to the Y axis of crystal I or the X axis of crystal II and propagating

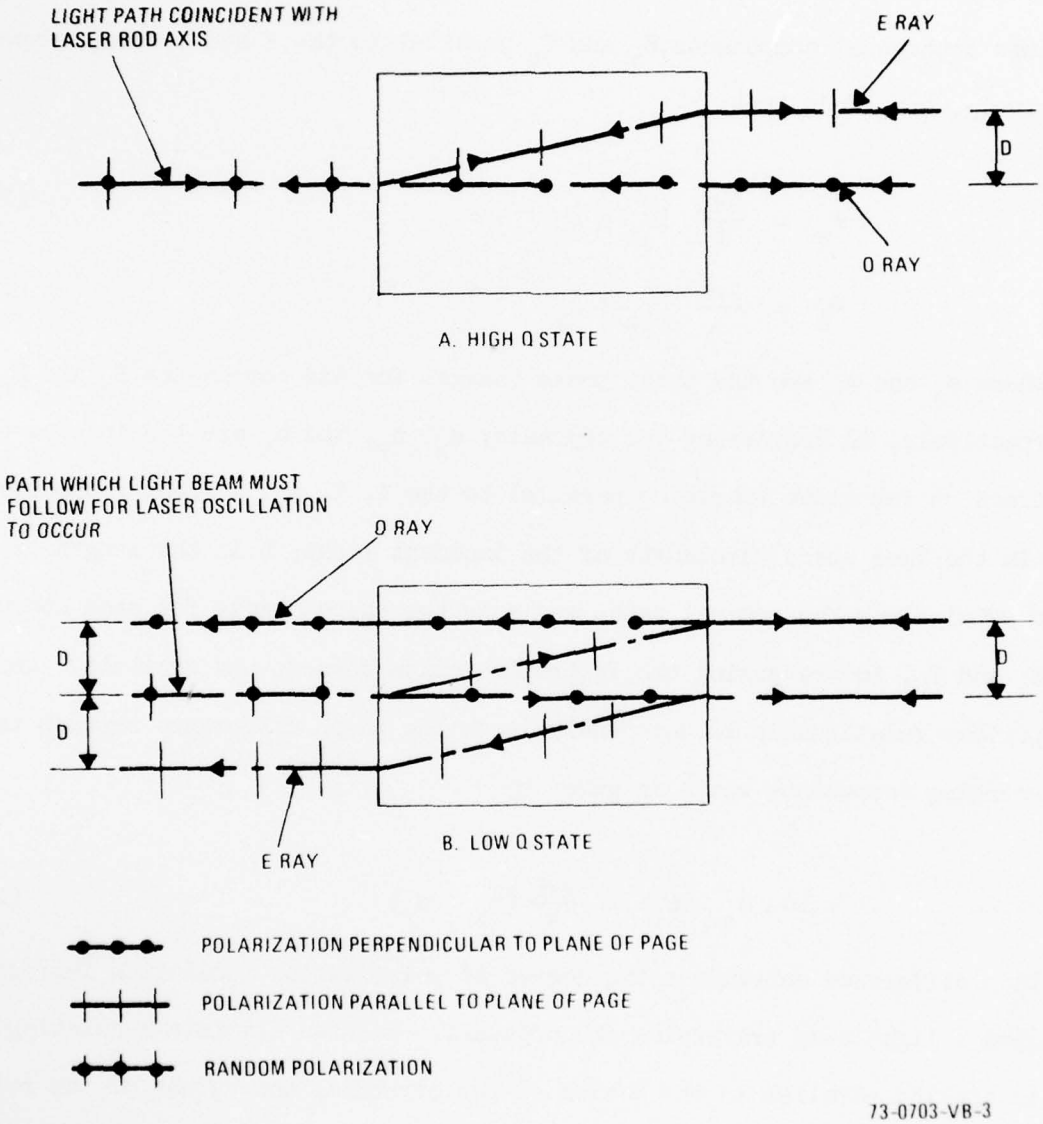

Figure 8 Extreme States of E/O Modulation Associated with Element B

along the optical path shown, the following relationships characterize the optical phase retardation induced by the crystals when subjected to an electric field parallel to the Z axis. Resolving the input light polarization into orthogonal components E_a and E_b parallel to the X and Y axes, respectively, one finds that

$$\phi_a = \frac{2\pi L}{\lambda} (n_z + n_x) + \alpha \tag{2}$$

$$\phi_b = \frac{2\pi L}{\lambda} (n_z + n_y) + \alpha \tag{3}$$

where ϕ_a and ϕ_b are the total phase changes for the components E_a and E_b, respectively, in traversing the crystals; n_x, n_y, and n_z are the indexes of refraction for light vibrating parallel to the X, Y, and Z axes, respectively; λ is the free space wavelength of the incident light; L is the length of each crystal along the optical path; and α is the phase change for each component, E_a and E_b, in traversing the isotropic medium between the crystals. An important relationship in this analysis is the phase difference between the emerging components which is given by

$$\Delta\phi = \phi_a - \phi_b = \frac{2\pi L}{\lambda} (n_x - n_y) \tag{4}$$

This difference determines the degree of polarization modulation impressed upon a light beam traversing the crystals. When an electric modulating field is applied parallel to the Z axes of the crystals, the values of the refractive indexes are given by

$$n_x = n_o \pm \Delta n$$

$$n_y = n_o \mp \Delta n$$

$$n_z = n_e = \text{constant}$$

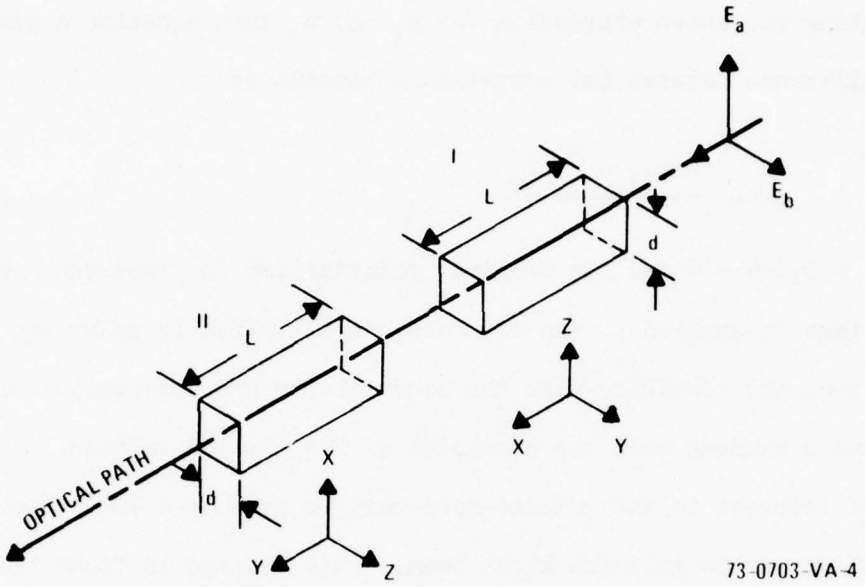

Figure 9 Orientation of E/O Crystals in Element QS

where

$$\Delta n = \frac{r_{63}\, n_o^{\,3}\, E_z}{2} = \frac{r_{63}\, n_o^{\,3}\, V_z}{2d} \qquad (5)$$

Δn = change in index of refraction as a function of applied field

n_o = ordinary index of refraction

n_e = extraordinary index of refraction

r_{63} = electro-optic coefficient

E_z = applied electric field

d = crystal thickness along Z axis

$V_z = dE_z$ = voltage applied parallel to Z axis of each crystal

Substituting the above expression for n_x and n_y into equation 4 gives the phase difference between the emerging components as

$$\Delta\Phi = \frac{2\pi r_{63} n_o^3 L V_z}{\lambda d} \tag{6}$$

With $V_z = 0$, $\Delta\Phi = 0$ and the original polarization is preserved. However, when voltage is applied to the crystals, an elliptically polarized wave emerges from the modulator with the eccentricity and orientation of major and minor axes dependent upon the magnitude of the applied voltage.

Of interest is the voltage necessary to produce a 90-degree rotation of polarization of the incident light beam. This voltage is found by setting $\Delta\Phi$ equal to π radians and solving for V_z. Solving equation 6 there is obtained

$$V_{\lambda/2} = \frac{\lambda}{2 r_{63} n_o^3} \cdot \frac{d}{L} \text{ Volts} \tag{7}$$

This voltage is known as the half-wave voltage since when applied it induces a 180-degree phase difference between the emerging components, E_a and E_b. In a double pass configuration, as would occur in the laser resonator, only the quarter wave voltage, given by

$$V_{\lambda/4} = \frac{\lambda}{4 r_{63} n_o^3} \cdot \frac{d}{L}, \tag{8}$$

is required to achieve a 90-degree polarization rotation because the optical phase retardation effect is cumulative. The principal advantage of this mode of polarization modulation is that it makes possible a reduction in the value of the switching voltage required (as compared to the fixed voltage requirements of a conventional E/O modulator), since with the two crystal transverse

field geometry the voltage necessary to obtain a given E/O modulation is proportional to the d/L ratio of the crystals.

3. E/O MODULATOR DRIVER

The E/O modulator used for the Cavity Dump-PTM laser uses Potassium Dideuterium Phosphate (KD^*P) crystals, each with a 10 mm square aperture and measuring 19 mm long. Quarter wave ($\lambda/4$) phase retardation occurs at an applied voltage of approximately 1700 volts. Figure 10 shows a schematic diagram of the driver circuit, used in conjunction with the modulator cell, which has been operated at PRF's up to 1 MHz with rise and fall switching times on the order of 5 and 10 nanoseconds respectively.

Referring to figures 1 and 10, operation of the modulator driver can be understood from the following discussion. At t = 0, the output coupling reflectivty for the resonant cavity is at R_o. This level is established by applying a fixed bias voltage (V_B) across the E/O modulator crystals (C_L) with tubes V1 and V2 biased off. The transition from R_o to 100% coupling reflectivity occurs when V1 is turned on for 5 nanoseconds by triggering avalanche transistor Q1 and discharging PFN 1* into the grid of V1. This causes plate current to flow in L1 which results in energy storage in this component. When V1 returns to the off state, the energy stored in L1 is transferred to the series combination of C3 and C_L which by resonant charging, causes the voltage at the plate of V1 to increase to approximately $2V_p$. C3 is adjusted such that the voltage of the plate of V2 is sufficient to produce a net voltage of zero across C_L. (Voltage on plate of V2 equals V_p during high Q time). This state

---

* Pulse Forming Network.

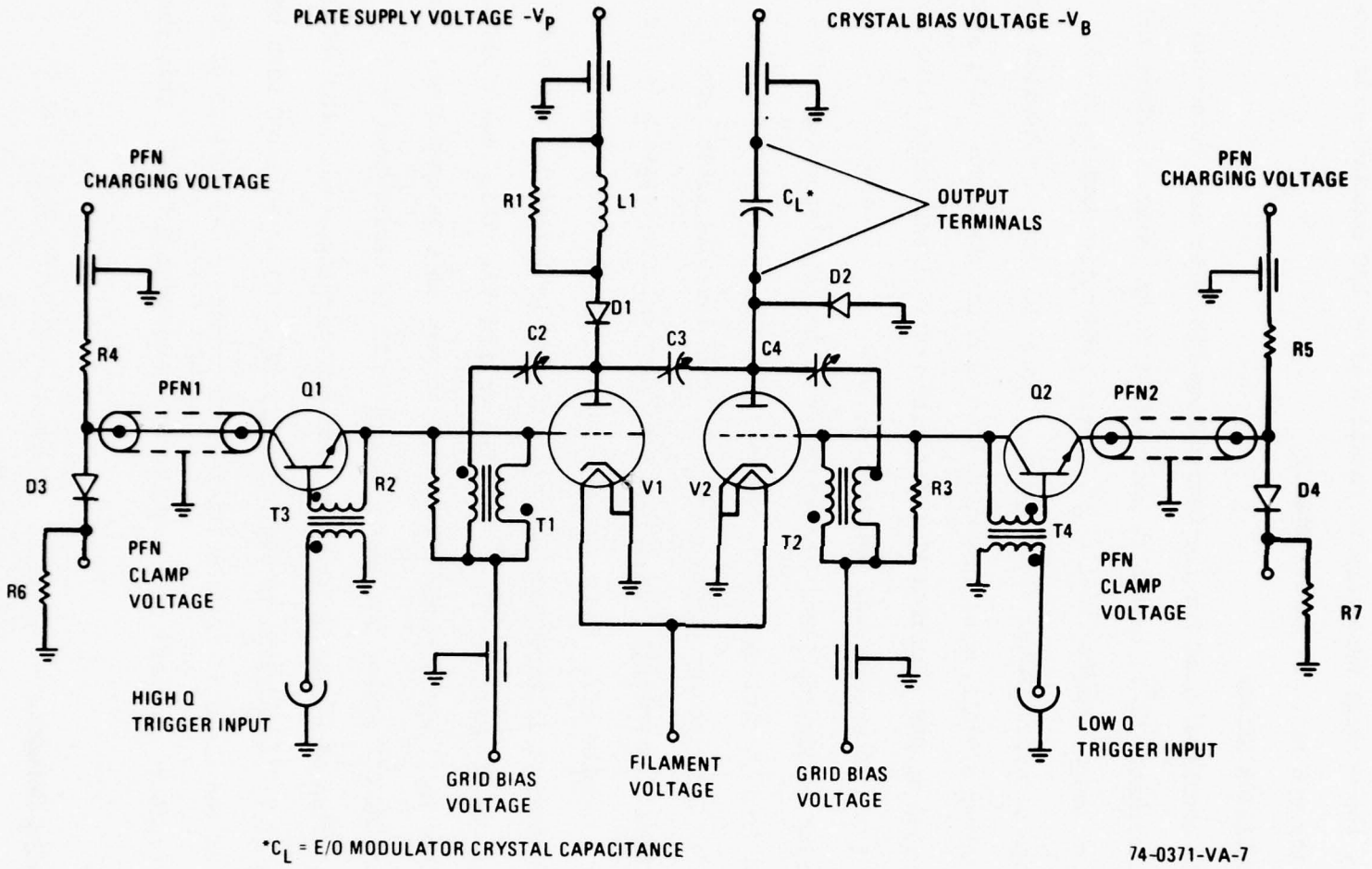

Figure 10 E/O Modulator Driver

corresponds to the high-Q condition of the laser resonator. Cavity Q remains high until time t_2 at which point tube V2 is turned on for 5 nanoseconds by triggering avalanche transistor Q2 and discharging PFN 2 into the grid circuit. The voltage on C3 does not change when V2 is turned on because the resonant charging voltage on C3 was sufficiently high to maintain D1 in a reverse biased condition; however, the voltage across C_L increases to return the output coupling reflectivity to R_o at time t_3. The Q-Switching cycle is repeated at t_4 when V1 is once again activated. Diode D2 provides a low resistance path for discharging C3 when V1 is turned on at the beginning of a cycle. Combinations C2, T1 and C4, T2 provide plate-grid neutralization of V1 and V2 respectively. R1 suppresses ringing in L1 during resonant charging.

SECTION III

EXPERIMENTAL PERFORMANCE EVALUATION

1. INSERTION LOSS OF RESONANT CAVITY ELEMENTS

The insertion loss of resonant cavity optical elements is extremely important for the Cavity Dump-PTM laser system. Significant levels of loss not only reduce overall system efficiency but can also produce average power and pulse-to-pulse amplitude instabilities. As diagramed in figure 7, the three major intracavity elements are the laser rod, calcite polarization separator, and E/O modulator.

a. Laser Rod

Aside from its normal loss coefficient,* there are two principal loss mechanisms of importance associated with the laser rod:

1. Scattering at the antireflection coated end faces.
2. Internal refractive index variations produced by pump lamp and coolant flow spatial instabilities.[8]

Although the absolute magnitude of the losses associated with the above two mechanisms is normally low, and their resultant effect on overall efficiency negligible, they can significantly influence operational stability for a high order mode laser. Therefore, the laser rod end faces, as well as all other optical surfaces within the resonator through which the beam passes, have

---

* Normal loss coefficient, β, for YAG: Nd has a typical value of .005cm^{-1}.

been specified for lowest possible scattering. Also special care was taken in the design of the cooling configuration to prevent random fluctuations in the coolant flow pattern across both the rod and the pump lamp.

b. Calcite Polarization Separator

The calcite polarization separator utilized for the Cavity Dump-PTM laser measures .6 x 1.8 cm, at each polished end face, by 5.4 cm long. Anti-reflection coatings are applied to each face to minimize losses. Figure 11 illustrates the lasing efficiency obtained with and without the calcite polarization separator in the resonant cavity; output coupling reflectivity was 95%. Based on these data, a single pass loss of .75% (including reflection losses) is calculated for this element. This result clearly illustrates that the intrinsic absorption loss in calcite, even for a path length of 5.4 cm, is quite low at 1.06 micrometers.

c. E/O Modulator

The E/O modulator design incorporates two BK-7 windows, antireflection coated at the glass-air interface, two KD*P cyrstals each measuring 15 mm in length, and a thin quartz spacer. Reflection losses are minimized by employing index matching liquid films between the various elements within the cell.

Initially it was intended to use Freon 214 as the index matching liquid in the E/O modulator cell. Prior testing of this liquid indicated an excellent index matching capability as well as extremely low absorption at 1.06 micrometers. The original samples of Freon 214 were obtained from DuPont which no longer manufactures this product. During the present program, we were unable to obtain sufficiently pure samples from secondary sources; as a result, several possible replacement liquids were investigated.

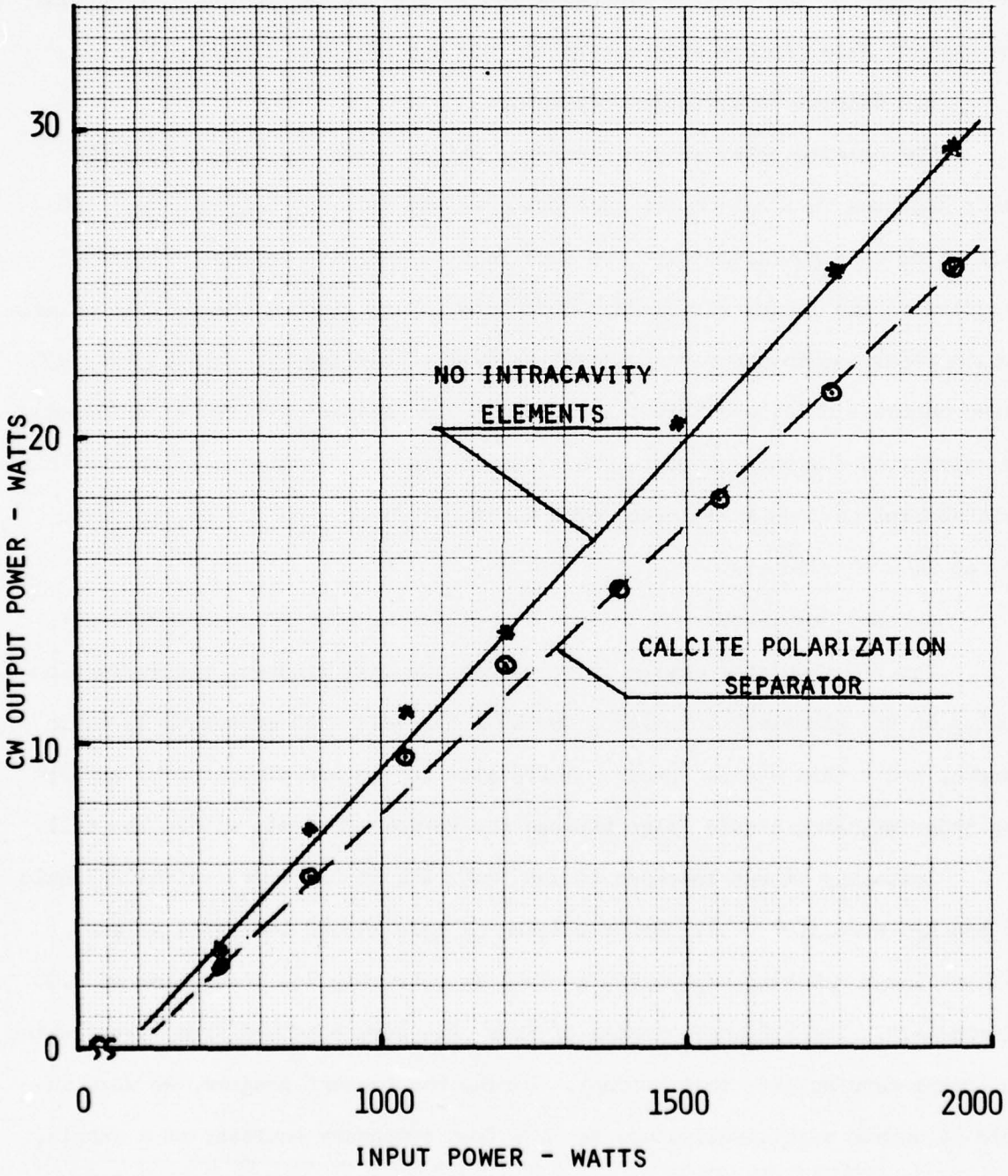

Figure 11 Insertion Loss Data with 95% Coupling Reflectivity: Calcite Polarization Separator

Figure 12 illustrates the lasing efficiency obtained when samples of the various test liquids were inserted in the resonant cavity. The liquid samples were obtained by allowing capillary films to form between the uncoated faces of two modulator cell windows placed in light contact with each other.

Tests with Freon E-3*, which is commonly employed as an index matching fluid in E/O Q-Switches for pulse pumped lasers, indicated that severe output power and mode instabilities could be expected when the average circulating power density exceeded 3 kilowatts/cm^2. The source of instability appears to be temporal variations in the refractive index of the E-3 due to absorption of the 1.06 micrometer radiation. The results of figure 12 have been used to calculate an effective single pass transmission loss of 2.5% for the Window/E-3/Window test sample.

For the liquid group consisting of Coolanol 25, DC550, DC510, and OS59**, experimental data fell within the band indicated in figure 12. Within this band, single pass loss for all window-liquid-window combinations was calculated to be 1.3 to 1.5%. Of these four liquids, DC510 showed a somewhat lower loss and in a capillary film did not influence the stability of the oscillating TEM_{nm} modes even at high circulating power levels; DC 510 was employed in the final E/O modulator assembly.

---

* Freon E-3 is manufactured by E.I. DuPont

**Coolanal 25 and OS59 are manufactured by Monsanto; DC 510 and DC550 are manufactured by Dow Corning.

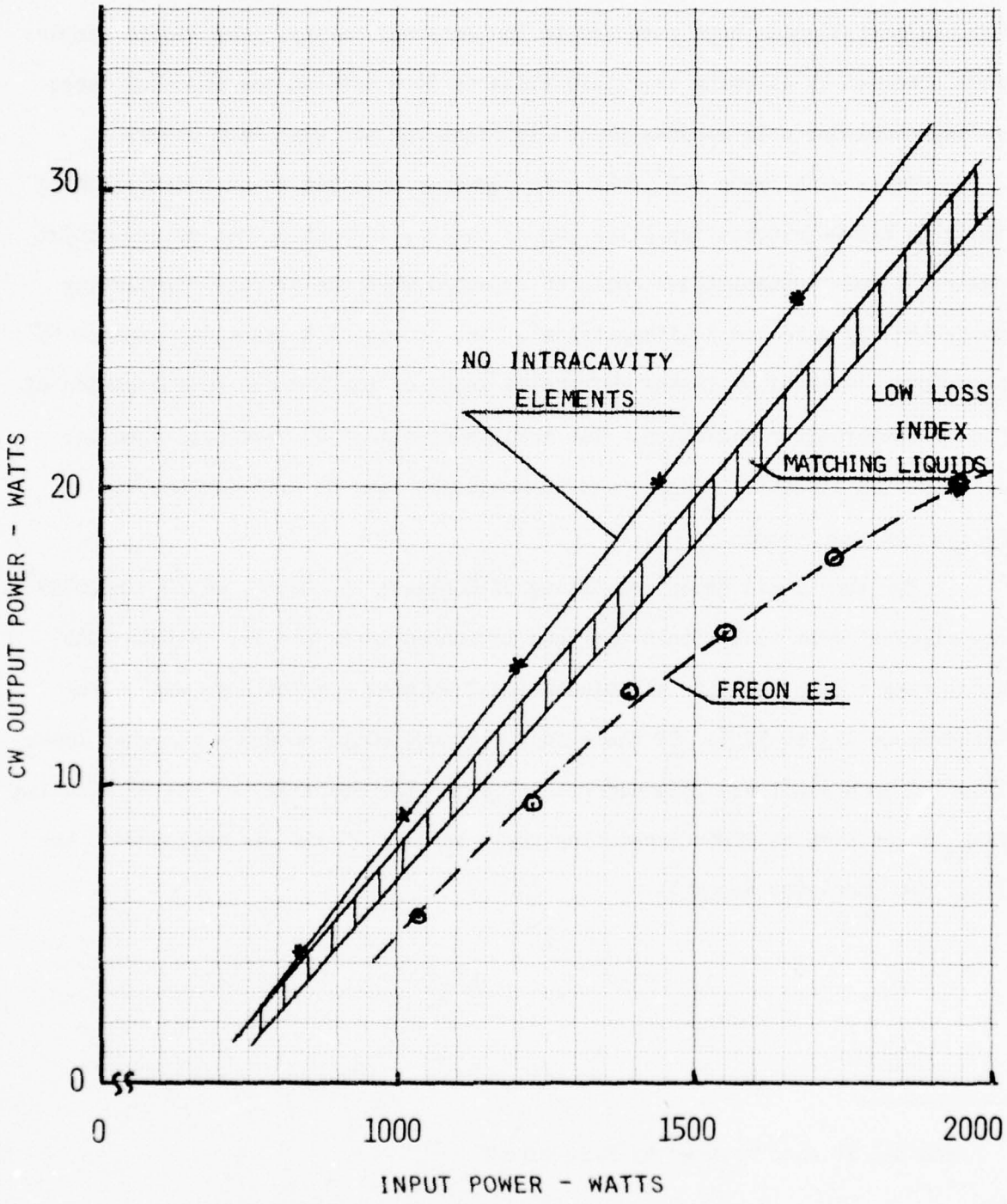

Figure 12 Insertion Loss Data with 95% Coupling Reflectivity: Index Matching Liquid Between Two Windows

Figure 13 illustrates the progressive loss in lasing efficiency incurred as E/O modulator elements were added to the resonant cavity. As indicated above, a capillary film of DC510 between two BK-7 windows introduced a single pass loss of 1.3%; addition of a thin fused quartz spacer (plus an additional film of DC510) increased the single pass loss to 3%; replacement of the spacer element with a single 15 mm long crystal of KD*P changed the single pass loss to approximately 5.3%.*

Analysis of the above data indicated that the quartz spacer was of poor optical quality. Efficiency obtained with the KD*P crystal was particularly low and represented a single pass loss for this KD*P crystal was particularly low and represented a single pass loss for this single element of 4%. Although the KD*P crystal utilized in the preliminary test was "fully" deuterated, the actual deuteration level was unknown. Since 1.06 micrometer absorption is strongly dependent on deuteration level, this factor may well account for the relatively low transmission observed. Were the elements tested above employed to construct an E/O modulator as described at the beginning of this section, the single pass loss for the modulator would be approximately 10%; this level of insertion loss is unacceptable for a low gain CW laser.

Insertion loss measurements were also obtained using an antireflection coated "fully" deuterated KD*P crystal. This crystal measured 1.78 cm in

---

* KD*P crystal obtained from INRAD

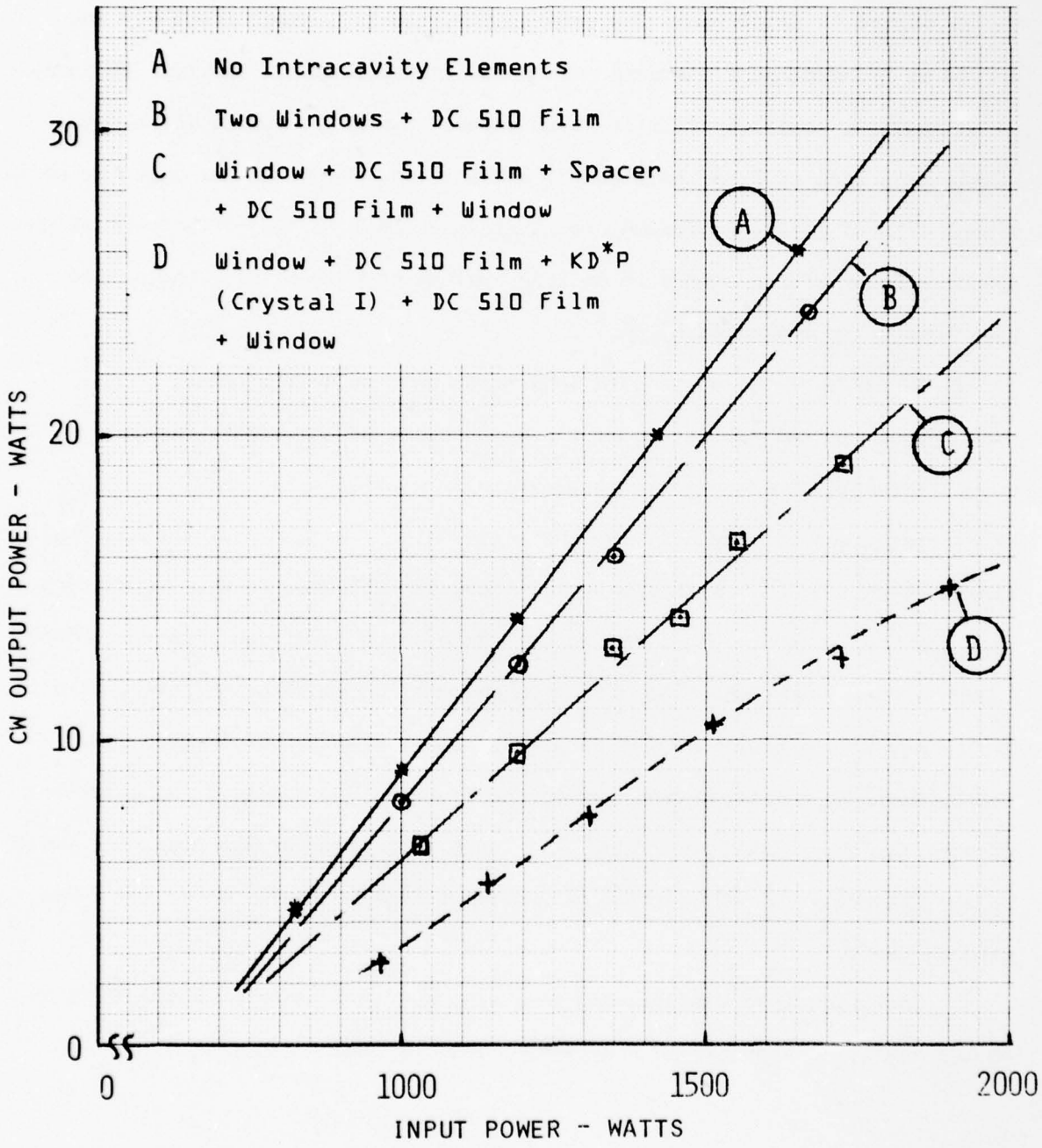

Figure 13 Insertion Loss Data with 95% Coupling Reflectivity: Modulator Elements

length, was obtained from Isomet Corp. in 1971, and had an unknown deuteration level. Experimental results are given in Figure 14. Data were recorded with and without a metallic heat sink applied to the four crystal sides. Curves A and B in Figure 14 were obtained using a 95% output reflector and appear to manifest a gradual roll-off in efficiency as the input power increases. Single pass crystal transmission was calculated from these curves and is plotted in Figure 15. Power dependent losses are obviously decreased when the crystal is coupled to a heat sink. In addition, the initial insertion loss (low power) of the Isomet crystal was lower than that of the INRAD (Figure 13) crystal by an approximate factor of 2:1.

2. MODULATED LASER PERFORMANCE

a. Modulated and Unmodulated Power Efficiency

Efficiency of the final resonator configuration is illustrated in Figure 16. Modulator construction was as described in Section III.1.a; however, a different pair of KD*P crystals than those previously tested (see Figure 13) were employed.* CW efficiency was measured by biasing the E/O modulator cell at a fixed voltage and maximizing the CW output at each input power level. Modulated output power was measured at a PRF of 100 KHz and a pulse amplitude fluctuation level of $\pm$10% (See Section III.2.d).

From the data in Figure 16, the best recorded ratio of modulated to unmodulated output power was approximately .85. This ratio fell off to a minimum value of .75 as output power was increased. Since power was measured

---

* These crystals were also obtained from INRAD

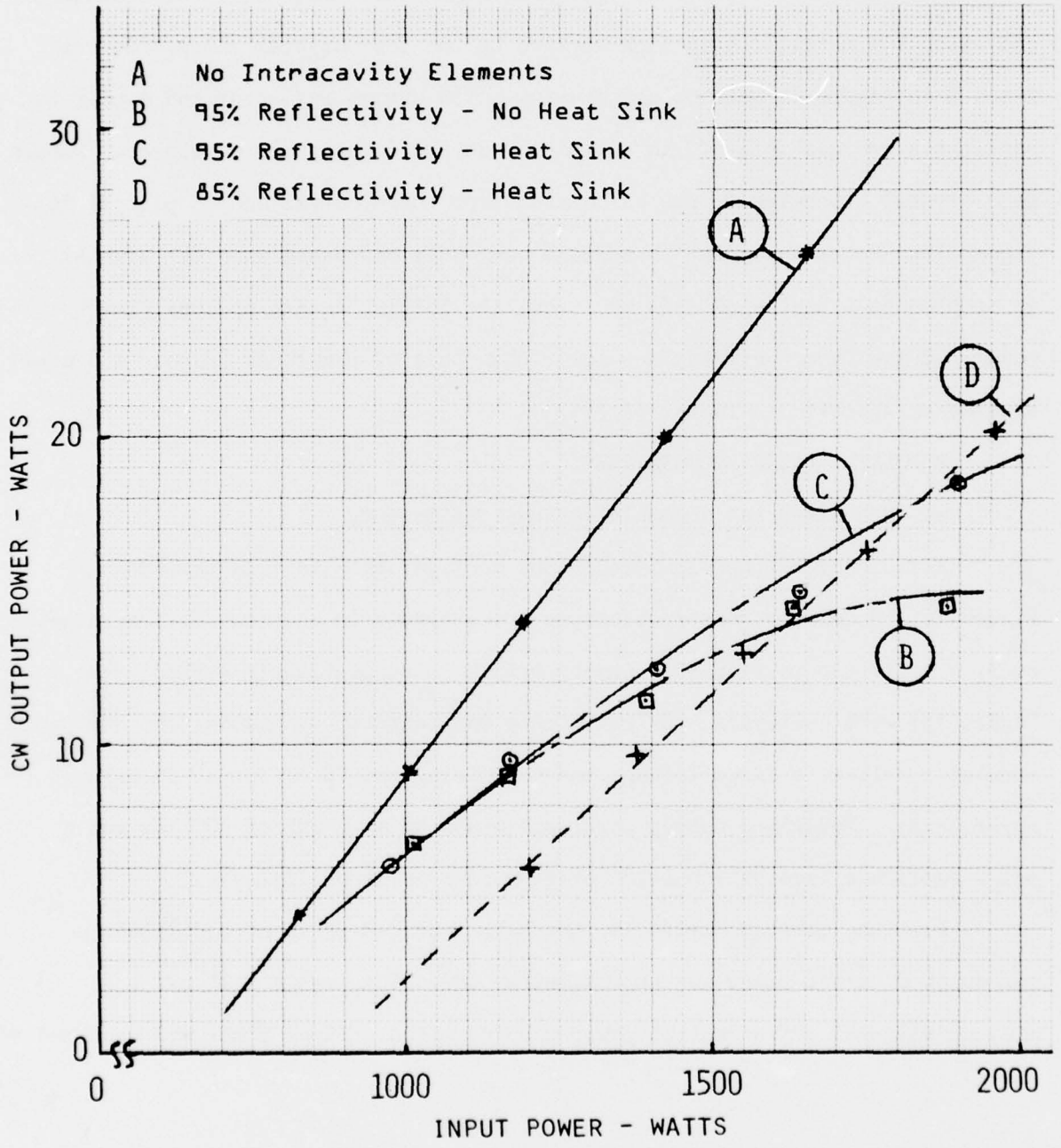

Figure 14 Insertion Loss Data for Antireflection Coated Crystal of KD*P

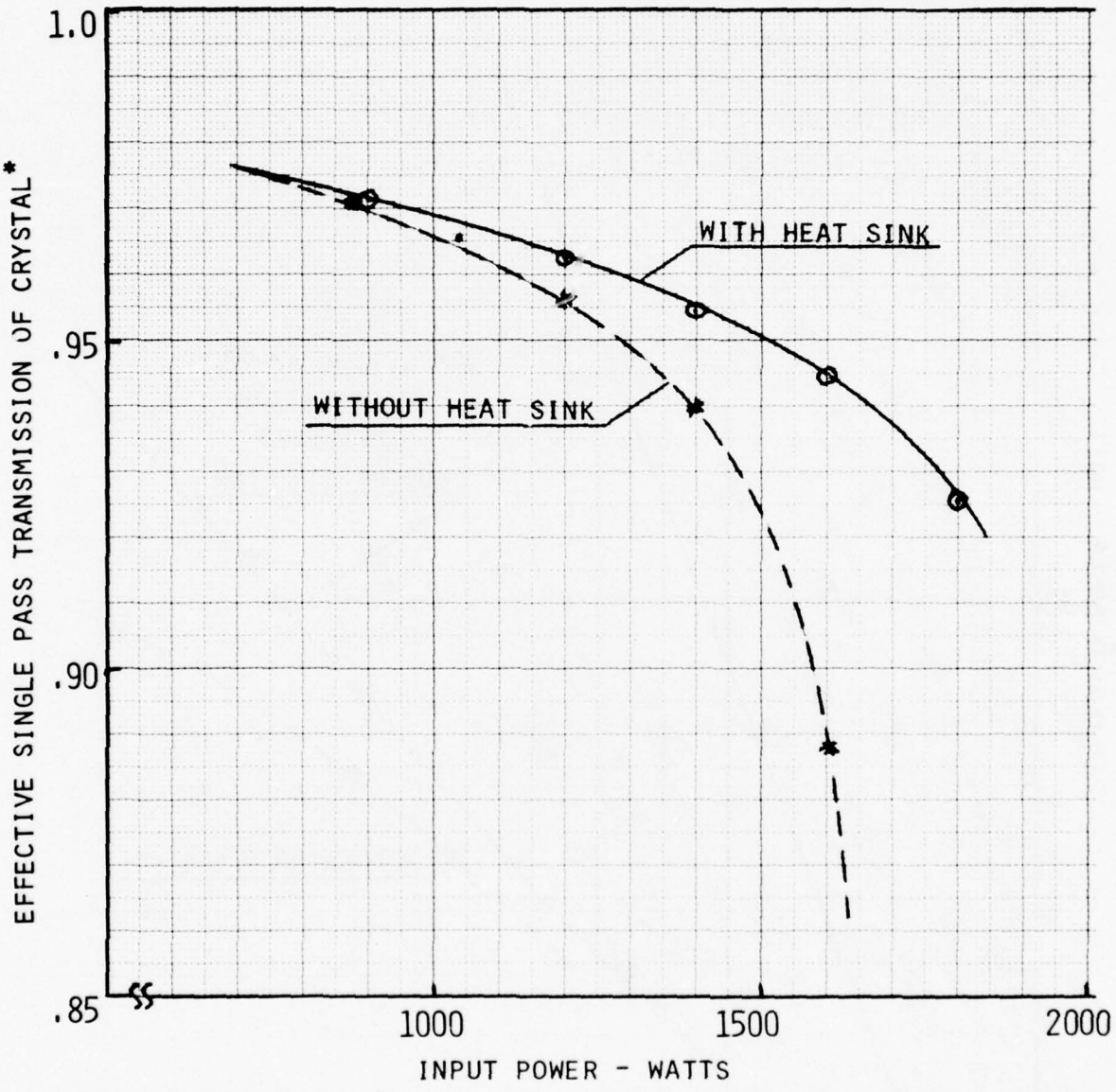

* Includes losses at antireflection coated interfaces

Figure 15 Single Pass Transmission of Antireflection Coated Coated Crystal of KD*P

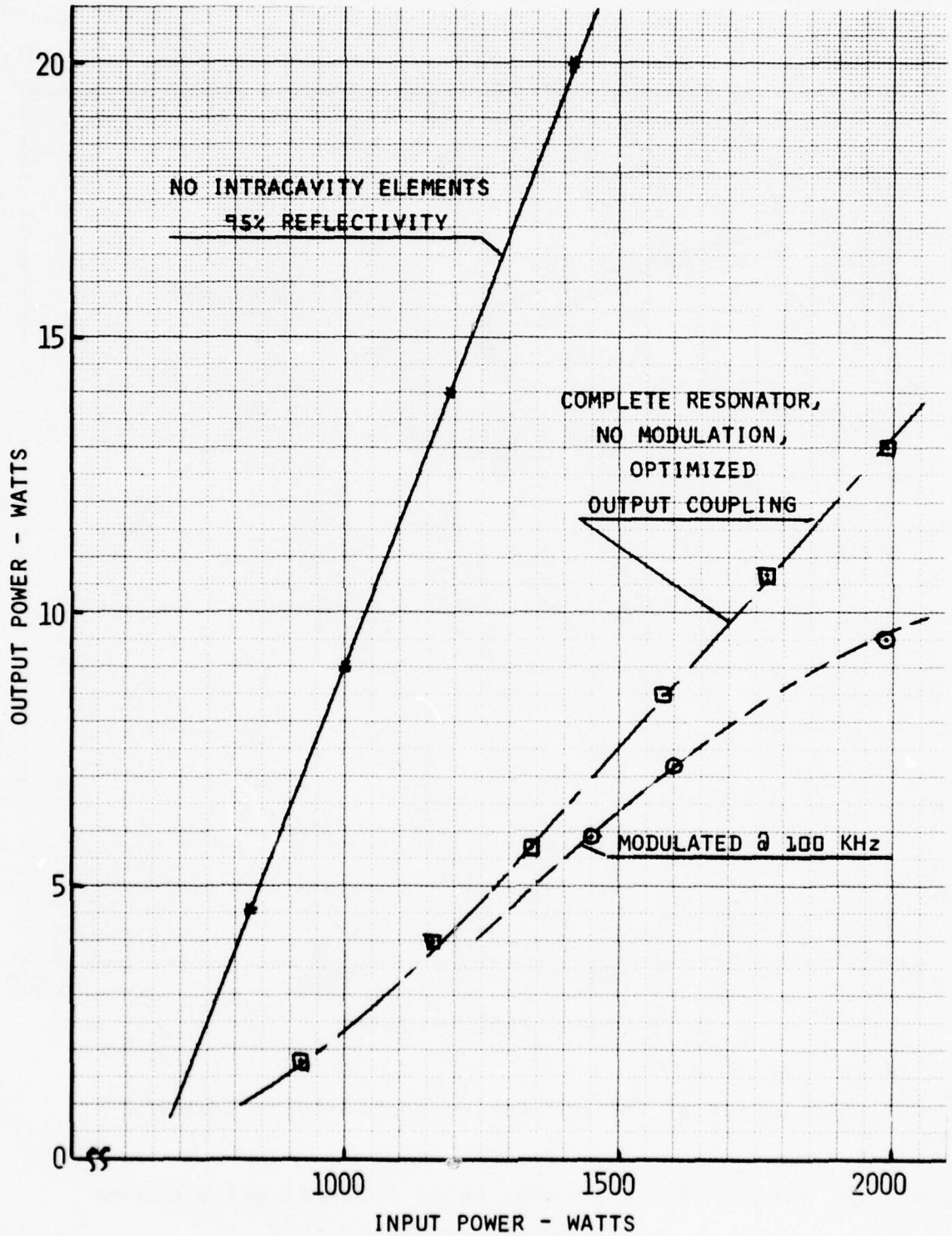

Figure 16 Final Resonator Efficiency

at a constant pulse amplitude stability, and it was observed that TEM_{nm} mode stability decreased with increasing output power, this performance is consistent with expected behavior as discussed in Section III.2.d.

Extended PTM operation is important primarily because it offers a technique to bridge the frequency gap between PTM and CD modulation without sacrificing overall laser efficiency (See Section II.1). Measurements were made of average output power for PRF's between 100 KHz and 1 MHz; pulse amplitude stability was maintained at a constant level. Observation of pulse dynamics indicated that 100 KHz was the approximate transition point between PTM and Extended PTM modulation. Extended PTM modulation was required up to and including 1 MHz. Over the 100 KHz to 1 MHz range, no frequency dependent change in output power was recorded.

b. Output Pulse Width

Output pulse width was recorded over the 100 KHz to 1 MHz PRF range and at various levels of output power. Figure 17 is a photograph of the superposition of multiple output pulses as recorded on a Tektronix 585 oscilloscope; pulse amplitude stability is clearly shown. As expected, the temporal shape of the output pulse was found to be essentially independent of PRF and power level.

Prior to modulator driver construction, a computer simulation was utilized to establish that a low Q coupling reflectivity (R_o in Figure 1) of 50% would provide satisfactory pulsed operation. This finding resulted in a substantial decrease in modulator electronics complexity but its implementation increased the fall time of the laser output pulse. Even with this modification, however, half intensity pulse width was approximately 40 nanoseconds.

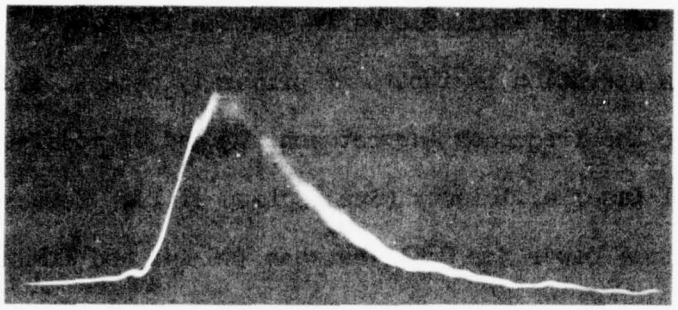

Figure 17 Output Pulse Waveform: 20 ns/div.

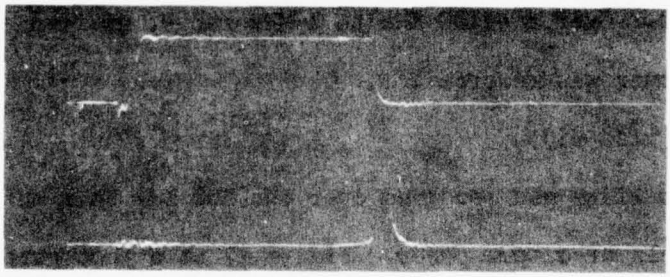

Switching Waveform

Output Pulse

Figure 18 E/O Modulator Switching Waveform with Output Pulse 200 ns/div.

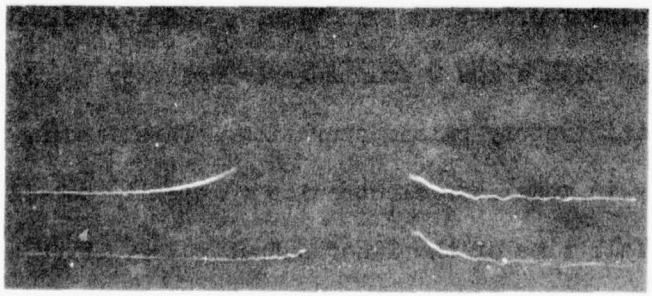

Switching Waveform

Output Pulse

Figure 19 Output and Intra-Cavity Laser/Waveforms: 40 ns/div.

c. Pulse Formative Characteristics

Figure 18 illustrates laser pulse emission in relationship to the E/O modulator switching waveform. Pulse formative time, defined as the time between t=o and $t=t_2$ in Figure 1, slowly increased as the PRF varied from 100 KHz to 1 MHz but remained less than 1 microsecond for typical operating power levels.

Lasing intensity at the laser output is compared to the lasing intensity internal to the resonator in Figure 19. The upper trace is the resonator internal intensity and shows the characteristic exponential buildup of the photon density. Output pulse formation is shown in the lower trace; pulse rise time is essentially established by the E/O modulator switching characteristics while the fall time approximates an exponential cavity photon decay through a 50% output coupling reflector.

Figure 20 illustrates the relationship between modulator switching waveform and pulse output as a function of PRF; average output power was 3.0 watts. From these data the modulator duty cycle, defined as the ratio of high Q dwell time to total PRF period, was calculated. Duty cycle as a function of PRF is plotted in Figure 21.

d. Pulse Amplitude Stability

For simplicity, the rate equation analysis used to generate the preliminary data on Extended PTM operation (as presented in Section II.1) ignored the contribution of spatially varying gain and loss, across the laser rod aperture, to operational stability. Such a spatial dependence arises naturally from non-uniform pumping of the rod and from laser radiation field variations associated with the oscillating TEM_{nm} modes. Pulse to pulse amplitude stability for Extended PTM operation depends primarily on the ability to reproduce a given level of inversion (at a fixed PRF) when the cavity Q is switched

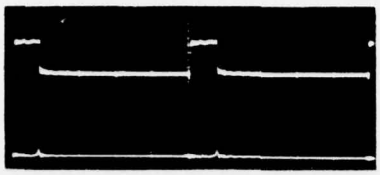

20.a 102 KHz - 2 μs/div.

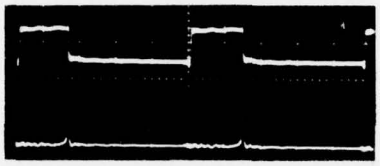

20.b 213 KHz - 1 μs/div.

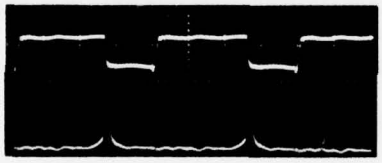

20.c 511 KHz - .5 μs/div.

20.d 765 KHz - .5 μs/div.

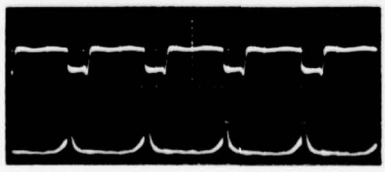

20.e 931 KHz - .5 μs/div.

Figure 20 E/O Modulator Switching Waveform and Output Pulse vs PRF

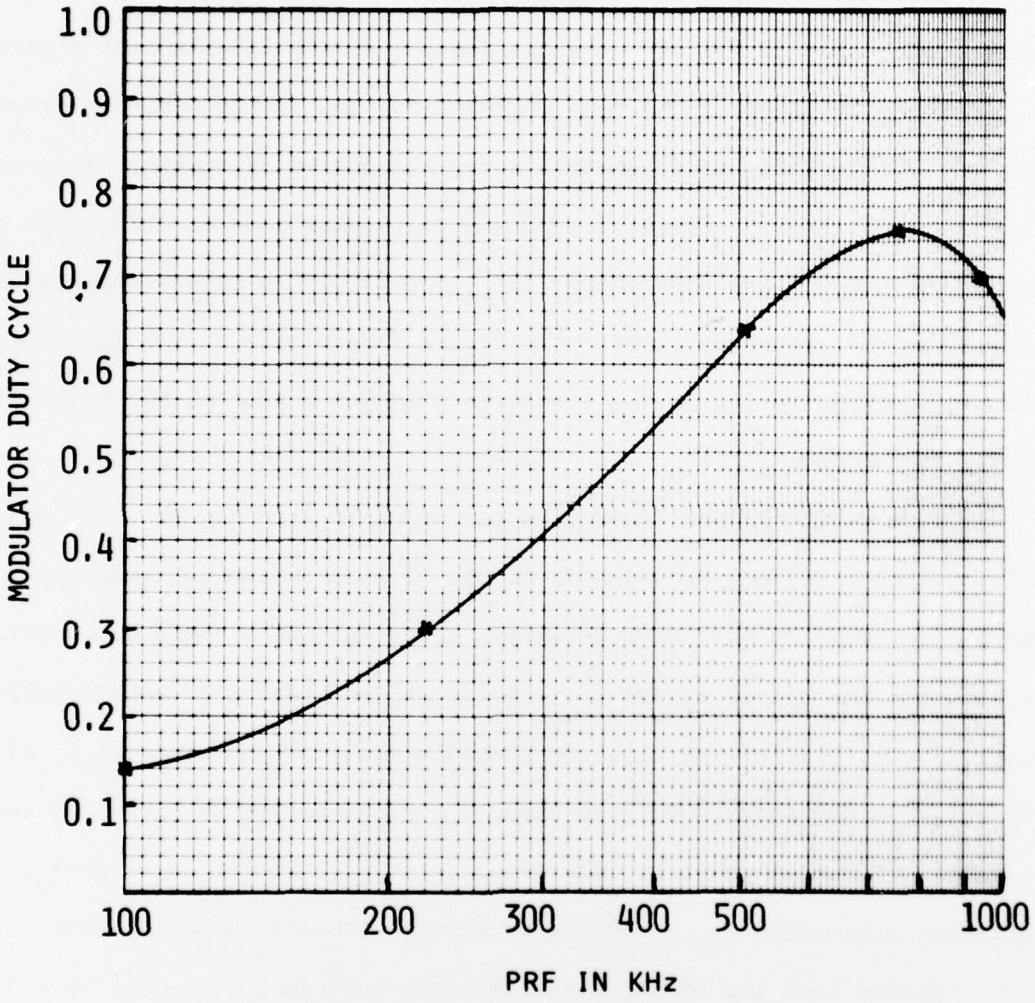

Figure 21 Modulator Duty Cycle vs PRF at Average Power Output of 3 Watts

from minimum to maximum at the beginning of each pulse formative cycle (t_1 in Figure 1). Gain level, in turn, is determined by pump rate, cavity losses, and the magnitude of photon flux at the time the laser pulse is switched out of the resonant cavity (t_2 in Figure 1). Strictly speaking, constant amplitude pulses occur only if all of the above factors remain invariant at a given PRF.

For a CW laser of the type employed for the Cavity Dump-PTM program, the oscillating TEM_{nm} modes exhibit a certain degree of spatial cross-coupling (ie, the laser energy extracted from any particular mode is influenced by the lasing characteristics of adjacent TEM_{nm} modes). This cross-coupling is enhanced for the resonator geometry in Figure 7 by virtue of the fact that pump induced thermal lensing in the laser pod produces a spatial mixing of circulating radiation.

At a given PRF the low Q time period (t_4-t_3) in Figure 1 was adjusted until output waveforms as shown in Figure 17 were obtained. This waveshape was a compromise between average output power and pulse amplitude stability. At this optimum point, assume $(t_4 - t_3) = \Delta t_o$ and that the average pulsed power output, p_o, is less than the unmodulated CW output power p_{cw}. If $(t_4 - t_3)$ is adjusted to be less than Δt_o, pulse amplitude stability improves somewhat but output power rapidly drops below p_o. For $(t_4 - t_3) > \Delta t_o$, output power approaches p_{cw} but pulse amplitude stability deteriorates.

Assume that the PRF is fixed and that initially $(t_4 - t_3)$ is adjusted small enough that no laser pulses are emitted. As $(t_4 - t_3)$ is slowly increased, a condition is reached where pulsed oscillations can be supported in the lowest order TEM_{oo} mode.* At this point pulse amplitude stability is

* The TEM_{oo} is the first to oscillate not only because of its lower loss but also because gain is maximum in the center of the laser rod.

excellent but average power output is considerably below p_{cw}. A further increase in $(t_4 - t_3)$ progressively permits additional lower order modes to oscillate, but the optimum condition for TEM_{oo} oscillations no longer exists and a certain degree of pulse amplitude instability ensues. As the number of oscillating modes increases, average output power and pulse instability simultaneously increase. A final operating point is reached, such as in Figure 17, by setting a maximum permissible amplitude fluctuation. For a given amplitude stability, the maximum power output, p_o, is primarily dependent on the spatial variation in pumping rate and the degree of TEM_{nm} Mode coupling; the greater the degree of mode coupling the larger the value of p_o.

As $(t_4 - t_3)$ increases above Δt_o, higher order modes toward the periphery of the rod begin to oscillate but the critical conditions of sustaining reasonably stable lower order mode oscillations are destroyed. Consequently, pulse stability deteriorates. If $(t_4 - t_3)$ is too small for a particular mode, no lasing energy can be extracted from that mode. If, on the other hand, $(t_4 - t_3)$ is greater than Δt_o, pulse amplitude will vary considerably for each interpulse period, but essentially all energy stored in inversion for a particular mode will be extracted as laser energy as long as the interpulse period is short compared to the fluorescent decay time constant. In light of this behavior, increasing $(t_4 - t_3)$ beyond Δt_o produces a power output which approaches p_{cw}.

3. PULSE PUMPED OPERATION

a. Power Supply Considerations

Design of the Cavity Dump-PTM laser power supply included the provision for pulsed pump operation. This mode utilizes the same D.C. arc lamp employed for CW pumping; pump PRF was 10 Hz with a 25% duty cycle (pump excitation period = 25 milliseconds). To maintain stable pulsed laser operation during the 25 millisecond pump period, it is necessary to provide a constant pump lamp output. Initially, the lamp parameters germane to satisfying this requirement were largely unknown and a study was undertaken to fully define the problem areas. As a result of this study, a technique for lamp pulsing was developed which provides a reasonably constant pump power during the pump burst as well as a 4000 watt* peak power capability. A block diagram of the final power supply is shown in Figure 22.

Figure 23 illustrates the measured volt-ampere characteristics of the Krypton arc lamp. After initial lamp start-up, lamp ignition is maintained between high power bursts by employing a simmer current of approximately 0.5 ampere (lamp voltage $\tilde{=}$ 100 volts). Switching to the high power state is initiated by applying a high current pulse (approximately 10 amperes) to the lamp in order to establish an intermediate operating point above the knee of the curve in Figure 23.

Observation of lamp current and output light intensity during switching transients strongly indicated that these two parameters track each other quite closely. Consequently, obtaining a constant pump intensity during the high power burst resolved itself into the problem of maintaining a square lamp current pulse in the face of a lamp impedance which essentially varies from 200 ohms during the interpulse simmer period to typically 1.9 ohms when lamp output power is a maximum.

* 4000 watt peak pump power to maintain a 25 watt average laser power output with 10 Hz, 25% duty cycle operation.

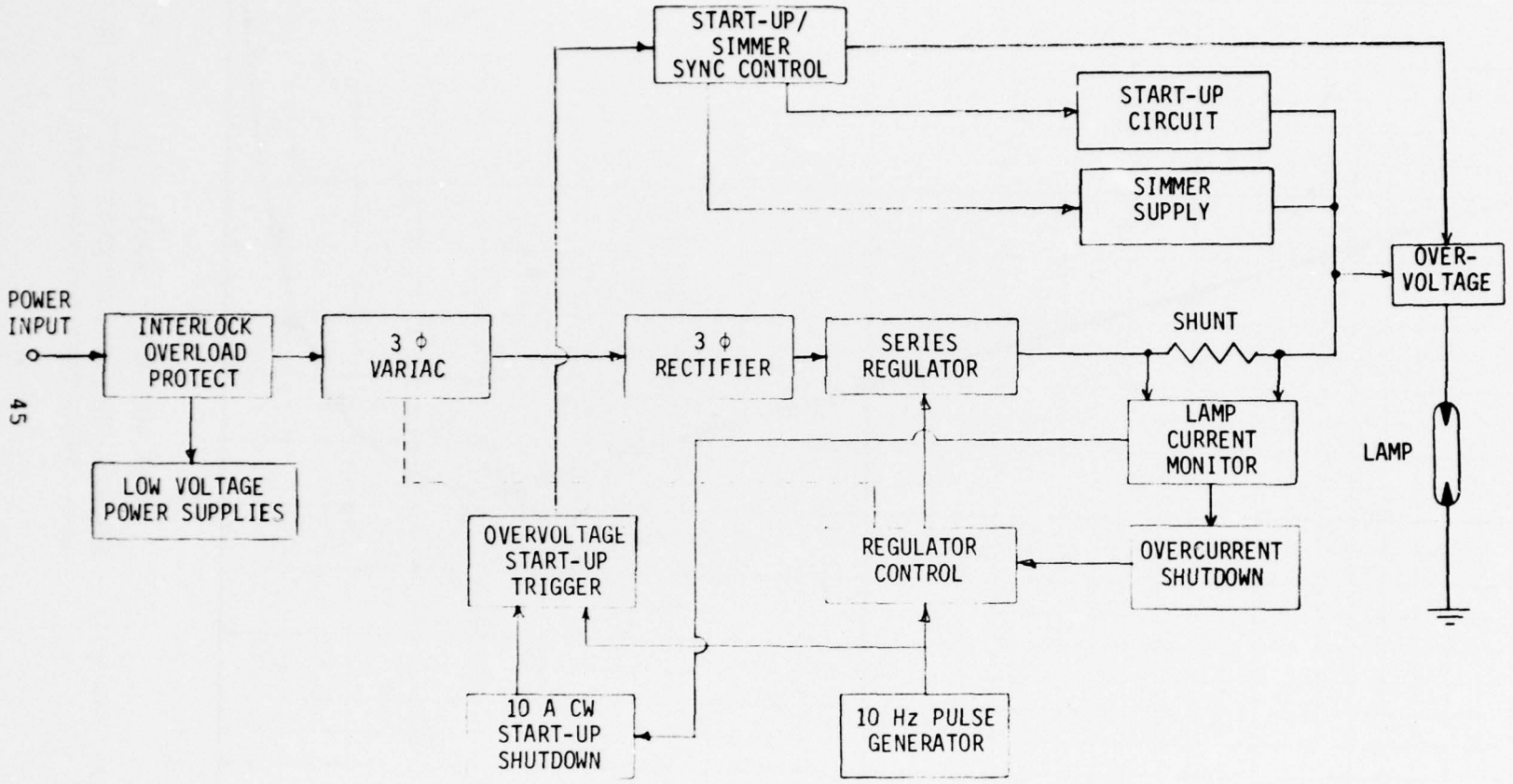

Figure 22 CW/Pulsed Power Supply Block Diagram

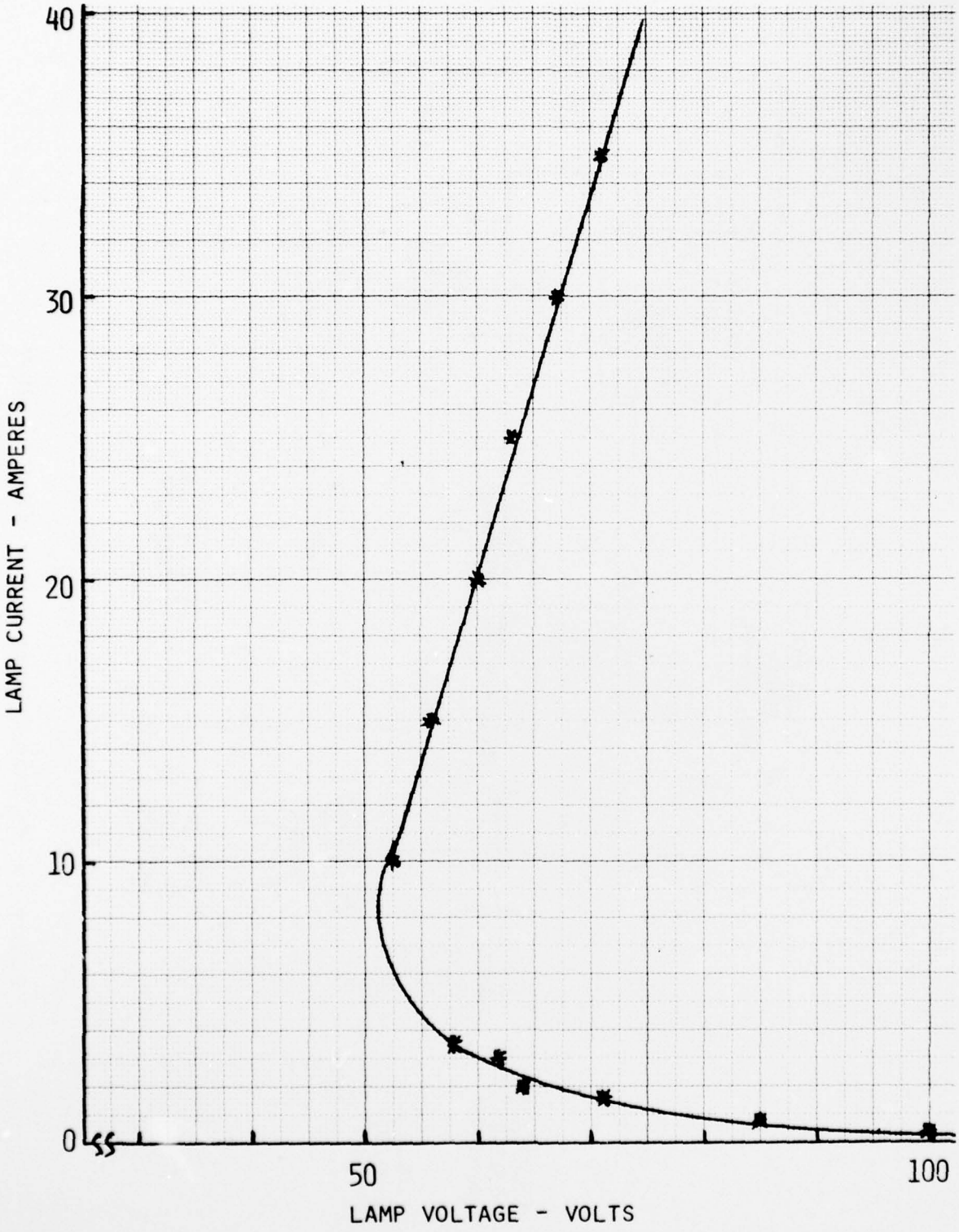

Figure 23 DC Volt - Ampere Characteristics of 5 mm bore, 50 mm arc, 3000 Torr Krypton Arc Lamp

Once above the knee in Figure 23, increased pump intensity is initiated by applying an elevated voltage pulse of approximately 180 volts peak across the lamp electrodes. This voltage rapidly decays in one millisecond to a lower voltage of 90 to 100 volts at which point the load is picked up by the primary high current supply. Voltage decay is tailored to provide a reasonably smooth transition from initial current rise to a steady state current condition. Even after the primary supply picks up the load, a slowly decreasing lamp voltage is required to maintain a constant lamp current. During the high power period, the lamp volt-ampere characteristics approach those given in Figure 23; however, 25 milliseconds appears to be an insufficient time for full plasma arc stability to be established. Light output waveforms for the final power supply design are illustrated in Figure 24.

b. Pulsed Laser Operation

Laser pulse characteristics during the pump burst period are essentially the same as discussed in Section 2. If the modulator duty cycle is adjusted for optimum pulse amplitude stability (approximately $\pm$ 10%) when the laser is operated CW at an average input power of p_o, switching to the pulse pumped mode, where the input power during the burst is p_o, also produces acceptable pulse stability.

At low average power levels, laser efficiency was found to be equivalent when switching between the CW and pulse pumped modes; if a CW input power p_o generates an average laser output power p_1, switching to pulsed operation, where the average input power is reduced to $p_o/4$, produces an average laser output power of $p_1/4$. As average output power increased, however, the pulse pump mode exhibited higher efficiency. For comparison with the DC pump data in Figure 16, peak pulsed pump powers (p_o) of 1080 and 1728 watts produced

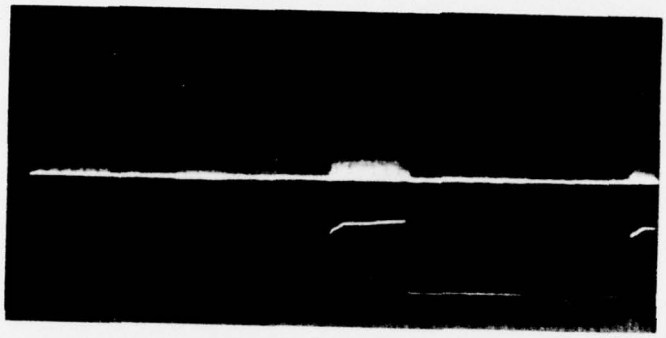

a. 20 ms/div.

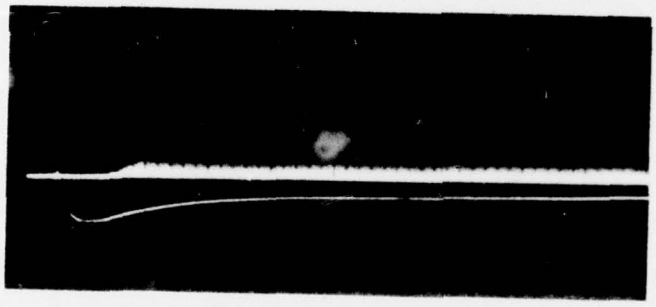

b. 2 ms/div.

Figure 24 Pulse Pumped Laser Output

peak laser powers (p_1) of 4.6 and 10 watts respectively. A maximum peak laser power of 22 watts at 100 KHz was recorded for pulse pumped operation during system tests.

A fundamental difference between CW and pulse pumped laser operation concerns the temporal buildup of the Q-switched pulse train during each pump period. We assume a delay, Δt, between the time the arc lamp is excited to its high power state and the first time the E/O modulator is switched from its low Q to high Q state ($t = 0$ in Figure 1). As stated in Section II.1.b, pulse-to-pulse amplitude stability is a maximum when the inversion at the beginning of each pulse formative time ($t = 0$ and $t = t_4$ in Figure 1) is identically reproduced at a given PRF. For our present discussion, we assume this value of inversion to be N_o.

At the beginning of the pump period, inversion builds in time according to the relationship

$$N = \tau KP \left[1-e^{-t/\tau}\right] \qquad (9)$$

when N is the inversion, τ is the fluorescent decay time constant, K is a pump efficiency constant, and P is the pump power during the pump period (here assumed to be constant). In the absence of modulation, N continues to build toward a maximum value of τKP ($t \rightarrow \infty$). A critical value of time, $t = \Delta t_c$, exists when $N = N_o$ such that the conditions for producing a constant amplitude laser pulse train are satisfied for the very first pulse. For Δt less than this critical value, pulse amplitude builds up on successive pulses until constant amplitude requirements are satisfied. Conversly, when $\Delta t > \Delta t_c$ the first Q-switched pulse exhibits an amplitude greater than the stable pulse

train amplitude with the result that inversion for the next pulse is less than N_o. After this first pulse, pulse amplitude builds in a way equivalent to the initial condition discussed above where $\Delta t < \Delta t_c$.

Figure 24 illustrates a typical buildup in pulse train amplitude as recorded for the Cavity Dump-PTM laser; PRF was 100 KHz, average power output was 1 watt. The value of Δt was adjusted such that no initial high energy pulse occurred and accounts for the fact that pulse train buildup closely follows temporal variations in the pump intensity. Pulse amplitude buildup time could be considerably reduced over that shown in Figure 24 by increasing the value of Δt to approximately 5 milliseconds. In this case, however, the pulse train is preceeded by an extremely intense single pulse; overall efficiency would also be reduced via increased fluorescent losses.

SECTION IV

CONCLUSIONS AND RECOMMENDATIONS

During contract F33615-74-C-1011, three major areas were investigated with regard to obtaining high PRF/high average power operation from a solid state YAG:Nd laser:

1. Application of high speed Electro-optic modulation techniques to a low gain CW pumped laser device.
2. Temporal modulation format required to obtain stable pulsed operation at PRF's between the classically accepted PTM and CD frequency limits.
3. Pulsed operation of a DC Krypton arc lamp at 10 Hz with a 25% duty cycle.

Electro-optic modulation of the laser output is provided by the combination of a double crystal transverse field polarization modulator and a calcite polarization separator. These elements permit efficient laser operation in the presence of high levels of laser rod birefringence. Use of the double crystal Pockels cell design provides the advantage of a relatively low quarter wave voltage ($\sim$ 1700 volts) as well as a high speed switching capability. The calcite polarization separator permits construction of a linear laser resonator which employs only two resonant reflectors and one polarization modulator.

Transmission of the calcite polarization separator was found to be excellent at 1.06 micrometers. Insertion loss measurements using the Pockels

cell modulator, however, indicated loss levels sufficiently high to produce a serious reduction in laser output power. The exact mechanism responsible for this loss is unknown at the present time but appears to be associated with absorption of 1.06 micrometer radiation in the $KD^{*}P$ modulator crystals and subsequent induced thermo-optic distortion in the optical path of the laser beam. This factor alone limited the maximum modulated output power obtained during this contract to 10 watts. Techniques to reduce optical losses associated with the E/O modulator should be investigated further. Improvements in this area will directly lead to a substantially increased modulated output power capability.

The validity of "Extended" PTM modulation, as discussed in Section II.a, has been substantiated during this contract. Laser modulation over the 100 KHz to 1 MHz range utilized this technique exclusively. At modulated output levels up to several watts, the ratio of modulated to unmodulated average power output was approximately .85; this value is reasonably consistent with that predicted by computational analysis. As output power increases this ratio tends to decrease, probably as a result of decreased TEM_{nm} mode stability.

Measurements of average modulated laser output power were obtained for a $\pm$10% pulse amplitude fluctuation. As discussed in the text, pulse amplitude stability can be traded off against average output power at a given PRF. Within the $\pm$10% stability limit, we obtained a maximum modulated output power of approximately 10 watts. In addition, average power output was found to be independent of PRF over the 100 KHz to 1 MHz range. Individual pulsewidths, as measured at the half intensity points, were on the order of 40 nanoseconds.

Since "Extended" PTM modulation has been found capable of providing efficient and stable pulsed operation, it should be relatively simple to provide a greatly increased PRF capability for the Cavity Dump-PTM laser. This increased range is accomplished by modifying the present modulator driver bandwidth. No changes in resonator geometry or temporal modulation format would be required. Below 100 KHz PTM modulation is applicable, beyond 1 MHz Cavity Dump (CD) techniques would be employed.

The Cavity Dump-PTM laser incorporates an arc lamp power supply which is switchable between DC and 10 Hz/25 percent duty cycle operation. In the DC mode, maximum input power to the lamp is 3000 watts. During the 25 millisecond pump burst, average lamp input powers on the order of 4000 watts have been achieved without damage to the lamp. Lamp life is maximized in the pulse mode by employing a sustaining or "simmer" current to maintain lamp excitation between high power bursts.

At a fixed input power level, switching the system between DC and pulse pumped modes produces a pump power during the burst equal to the DC power. CW or modulated laser efficiency as well as modulated laser pulse stability is essentially the same for DC and pulse pumped operation. In the pulsed pump mode, initiation transients associated with the formation of the laser pulse train can be controlled by varying the time delay between the initiation of the high power pump burst and the first Q-switched pulse of the sequence.

REFERENCES

1. C. H. Church and I. Liberman, Appl. Opt., 6, 1966 (1967)
2. G. D. Baldwin and I. T. Basil, IEEE J. Quant. Elect., QE-7, 179 (1971)
3. G. D. Baldwin, IEEE J. Quant. Elect., QE-7, 220 (1971)
4. J. L. Wentz, Proc. IEEE, 52, 716 (1964)
5. J. L. Wentz, Proc. IEEE, 60, 343 (1972)
6. A. J. DeMaria and G. E. Danielson, Jr., IEEE J. Quant. Elect., QE-2, p. 157 (1966)
7. K. Gurs and R. Muller, "Internal Modulation of Optical Masers," Proceedings of the Symposium on Optical Masers, New York: Polytechnic Press, 1963, pp. 243-252
8. T. Uchida, IEEE J. Quant. Elect., QE-1, p. 336 (1965)
9. R. B. Chesler and D. Maydan, J. of Appl. Ph7s., 42, p. 1028 (1971)
10. D. Maydan and R. B. Chesler, J. of Appl. Phys., 42, p. 1031 (1971)
11. A. A. Vuylsteke, J. of Appl. Phys., 34, p. 1615 (1963)